The Arabidopsis R-SNARE VAMP714 is essential for polarization of PIN proteins in the establishment and maintenance of auxin gradients

Xiaoyan Gu[1,2,*], Kumari Fonseka[1,3,*], Stuart A. Casson[1,4], Andrei Smertenko[1,5], Guangqin Guo[2], Jennifer F. Topping[1], Patrick J. Hussey[1] and Keith Lindsey[1]**

[1]Department of Biosciences, Durham University, South Road, Durham DH1 3LE, UK

[2]Ministry of Education Key Laboratory of Cell Activities and Stress Adaptations, School of Life Sciences, Lanzhou University, Lanzhou 730000, China

[3]Current address: Department of Crop Science, Faculty of Agriculture, University of Ruhuna, Mapalana, Kamburupitiya, Sri Lanka

[4]Current address: Department of Molecular Biology and Biotechnology, University of Sheffield, Firth Court, Western Bank, Sheffield S10 2TN, UK

[5]Current address: Institute of Biological Chemistry, Washington State University, Pullman WA 99164, USA

[*]These authors contributed equally to the work

[**]Corresponding author: keith.lindsey@durham.ac.uk

Word count main text: 4817

Summary: 200

Introduction: 492

M&M: 1350

Results: 2090

Discussion: 885

8 Main Figures, all in colour; 3 Supplementary Figures and 1 Supplementary video

Summary

- **The plant hormone auxin and its directional intercellular transport plays a major role in diverse aspects of plant growth and development. The establishment of auxin gradients in plants requires asymmetric distribution of members of the auxin efflux carrier PIN-FORMED (PIN) protein family to the plasma membrane. An endocytic pathway regulates the recycling of PIN proteins between the plasma membrane and endosomes, providing a mechanism for dynamic localization.**
- **N-ethylmaleimide-sensitive factor adaptor protein receptors (SNAP receptors, SNAREs) mediate fusion between vesicles and target membranes and are classed as Q- or R-SNAREs based on their sequence. We analysed gain- and loss-of-function mutants, dominant negative transgenics and protein localization of the Arabidopsis R-SNARE VAMP714 to understand its function.**
- **We demonstrate that VAMP714 is essential for the insertion of PINs into the plasmamembrane, for polar auxin transport, and for root gravitropism and morphogenesis. *VAMP714* gene expression is upregulated by auxin, and the VAMP714 protein co-localizes with ER and Golgi vesicles and with PIN proteins at the plasma membrane.**
- **It is proposed that VAMP714 mediates the delivery of PIN-carrying vesicles to the plasma membrane, and that this forms part of a positive regulatory loop in which auxin activates a VAMP714-dependent PIN/auxin transport system to control development.**

Key words

Arabidopsis thaliana, auxin transport, PIN proteins, R-SNARE, VAMP714

Introduction

The polarity of eukaryotic cells is associated with diverse aspects of cell differentiation and development, and one feature of this is the polar distribution of membrane proteins, such as to promote directional signalling or transport of molecules or ions. In plants, local biosynthesis and the regulated polar transport of auxin contribute to the generation of auxin gradients within tissues, necessary for spatially regulated gene expression and development (Reinhardt *et al*., 2000; Petrasek & Friml, 2009; Vanneste & Friml, 2009). Members of the PIN-FORMED (PIN) family of auxin efflux carriers accumulate in the plasma membrane on specific sides of the cell and determine the direction of auxin flow through tissues (Wiśniewska *et al*., 2006; Vieten *et al*., 2007).

Rapid changes in cell polarity involve clathrin-mediated endocytosis of PINs, dependent on both ARF-GEF (guanine-nucleotide exchange factors for ADP-ribosylation factor GTPases)- and Rab5 GTPase-dependent recycling (Steinmann *et al*., 1999; Geldner *et al*., 2001; Kleine-Vehn *et al*., 2008; Kitakura *et al*., 2011). Auxin itself inhibits this recycling, resulting in an accumulation of PIN proteins at the plasmamembrane, so promoting its own efflux (Paciorek *et al*., 2005). While the endocytic model accounts for the dynamic mobilization of PINs to different surfaces of the cell, it does not explain mechanistically how PIN proteins are delivered to the plasma membrane following their translation in the endoplasmic reticulum (ER).

Eukaryotes have evolved N-ethylmaleimide-sensitive factor adaptor protein receptors (SNAP receptors, SNAREs) as mediators of fusion between vesicular and target membranes. SNAREs can be grouped as Q- and R-SNAREs based on the occurrence of either a conserved glutamine or arginine residue in the centre of the SNARE domain (Fasshauer *et al*., 1998). In Arabidopsis, Vesicle-Associated Membrane Protein7-(VAMP7)-like R-SNAREs fall into two gene families - four VAMP71 group proteins are involved in endosomal trafficking (Uemura *et al*., 2004; Hong 2005) and eight VAMP72 group proteins are involved in secretion (Sanderfoot, 2007; Zhang *et al*., 2015). VAMPs have roles in abiotic stress tolerance (VAMP711, VAMP712; Leshem *et al*., 2010; Xue *et al*., 2018), in gravitropic responses (Yano *et al*., 2003), in cell plate formation (VAMP721, VAMP722; Zhang *et al*., 2011; Karnik *et al*., 2013; EI-Kasmi *et al*., 2013; Yun *et al*., 2013; Zhang *et al*., 2017; Uemura *et al*., 2019), in cytokinesis (Collins *et al*., 2003; Karnik *et al*., 2013), in defence responses (Kwon *et al*., 2008; Zhang *et al*. 2011, 2017), and in the transport of phytohormones (Dacks *et al*., 2002; Enami *et al*., 2009).

92 We identified a gain-of-function mutant of *VAMP714* following an activation
93 tagging screen in Arabidopsis (Casson & Lindsey, 2006). VAMP714 is structurally related
94 to VAMPs 711, 712 and 713, and previous data indicate that, while GFP fusions with
95 VAMP711, 712 and 713 localize to the vacuole in Arabidopsis suspension culture
96 protoplasts, GFP-VAMP714 co-localizes with the Golgi marker VENUS-SYP31 (Uemura
97 *et al*., 2004), but its function is unknown. In this paper, we use a combination of genetics,
98 trangenics and cell biological approaches to investigate the function of VAMP714.
99
100 **Materials and methods**
101 *Plant materials*
102 Wildtype *Arabidopsis thaliana* plants (ecotype Col-0) and activation tagging populations
103 (Casson & Lindsey, 2006) and growth conditions (Casson *et al*., 2009) have been described
104 previously. We identified two loss-of-function mutants of *VAMP714* from the SALK and
105 GABI-Kat collections of T-DNA insertion mutants (SALK_005917 and GABI_844B05;
106 www.signal.salk.edu), obtained from the Nottingham Arabidopsis Stock Centre
107 (Nottingham University, Sutton Bonington, UK). RT-PCR analysis showed that neither
108 mutant expresses the *VAMP714* gene to detectable levels. PCR was used to identify
109 homozygous insertion mutants among the GABI_844B05 F1 plants, using oligonucleotide
110 primers to amplify the *VAMP714* gene from wildtype but not from insertion lines: 5'-
111 CTGTTGTAGCGAGAGGTACCG-3' and 5'- AAGCATGTCAACAAGACCCTG-3'. To
112 confirm T-DNA insertion sites, a *VAMP714* primer (5'-
113 AAGCATGTCAACAAGACCCTG-3') and a T-DNA left border primer (5'-
114 ATATTGACCATCATACTCATTGC-3') were used to amplify the T-DNA flanking
115 sequence.
116 Genetic crosses between Arabidopsis plants were made under a Zeiss STEMI SV8
117 dissecting stereomicroscope (Carl Zeiss Ltd., Welwyn Garden City, Herts, UK) as
118 described (Souter *et al*., 2002). Arabidopsis seeds transgenic for the marker QC25 and
119 *DR5::GUS* were kindly provided by Prof. Ben Scheres (Wageningen University).
120 For hormone/inhibitor treatments of seedlings grown *in vitro*, *proVAMP714*::*GUS*
121 seedlings were germinated aseptically on growth medium and at 7 dpg were transferred to
122 growth medium containing auxin (indole-3-acetic acid, IAA) and, for comparison,
123 cytokinin (benzylaminopurine, BAP), the ethylene precursor ACC or the polar auxin
124 transport inhibitor 2, 3, 5-triiodobenzoic acid (TIBA) for a further 5 days before analysis.
125 For drug treatments, five-day-old seedlings were incubated in half-strength MS liquid

126 medium supplemented with 50 µM brefeldin A (50 mM stock in DMSO; Sigma-Aldrich),
127 and 20 µM latrunculin B (20 mM stock in DMSO; Sigma-Aldrich). DMSO in the same
128 final concentration (0.1%) was added to negative controls. Each treatment for confocal
129 imaging was repeated at least three times with similar results.
130
131 *Gravitropism assays*
132 Mutant and wildtype seedlings were grown on standard agar plates for 4 days and turned
133 to a 90° angle to measure the angle of bending towards gravity. The angle towards the
134 gravity was measured after 8, 12 and 24 h. The curvature of 20 seedlings for each genotype
135 was determined.
136
137 *Gene constructions, plant transformation and transient gene expression*
138 To create dominant negative mutant proteins, we expressed a non-functional fragment of
139 the VAMP714 protein expected to bind to the Qa, Qb and Qc complex of SNARE and
140 inhibit the binding of the native protein (Tyrrell *et al*., 2007). For constructing the dominant
141 negative gene construct, the longin and SNARE domains of the *VAMP714* gene sequence
142 were amplified without the transmembrane domain, using the oligonucleotide primers 5'-
143 GGGGACAAGTTTGTACAAAAAAGCAGGCTTCGTTGTAGCGAGAGGTACCGTG
144 -3', and 5'-
145 GGGGACCACTTTGTACAAGAAAGCTGGGTCCTATTAGCATTTTTCATCCAAAG
146 -3'. The amplified sequence was cloned directly into the pCR®2.1-TOPO vector
147 (Invitrogen, Paisley, UK) and then as an *Eco*RV fragment into the pDNOR207 Gateway
148 entry vector and then pMDC43 destination vector (Invitrogen, Paisley, UK), under the
149 transcriptional control of the CaMV35S gene promoter. qRT-PCR showed that the relative
150 abundance of the truncated transcript of *VAMP714* was higher in dominant negative
151 transgenics than is the native transcript in Col-0 wild type plants (Fig. S1). T4 transgenics
152 were produced by selfing, and at least 10 independent lines were analysed phenotypically.
153 To amplify the *VAMP714* promoter, the following oligonucleotide primer pairs
154 were used: 5'-GTCGAGCAGAGATCCTAGTTAGTGAGTCC-3' and 5'-
155 GTCGAGGTGATTCGATGACAGAGAGTGGAG-3'; the promoter PCR product was
156 cloned into pCR®2.1-TOPO and then as a *Sal*1 fragment into promoterless GUS reporter
157 binary vector pΔGUSCIRCE for *proVAMP714::GUS*.
158 For the *pro35S::VAMP714:GFP* fusion protein, the coding region was amplified
159 using primers 5'-TTAATTAACGCGATTGTCTATGCTGTTGTAGCG-3' and 5'-

160 CAGATTTTAAGATCTGCATGATGG-3', and the product was cloned into the pBIN-
161 GFP vector (Dr. David Dixon, Durham University). For *proVAMP714::VAMP714:CFP*
162 and *proVAMP714::VAMP714:mCherry*, a ca. 3.5 kb genomic fragment, comprising ca. 2
163 kb promoter and 1.5 kb coding sequence of the *VAMP714* gene, was amplified using
164 primers 5'-
165 GGGGACAAGTTTGTACAAAAAAGCAGGCTCAGAGATCCTAGTTAGTGAGTCC
166 -3' and 5'-
167 GGGGACCACTTTGTACAAGAAAGCTGGGTCAGATCTGCATGATGGTAAAGTG
168 -3'. The PCR product was cloned into pCR®2.1-TOPO vector and then as an *Eco*RV
169 fragment into the pDNOR207 Gateway entry vector and then pGHGWC destination vector.
170 All constructs were validated by sequencing.
171 Transgene plasmids were introduced into *Agrobacterium tumefaciens* C58C3 by
172 triparental mating, and plant transformation was performed by the floral dip method
173 (Clough & Bent, 1998). Transformed plants were selected using standard growth medium
174 supplemented with kanamycin (50 µg/ml for *proVAMP714::GUS*), Basta (15 µg/ml for
175 *pro35S::VAMP714:GFP*) or hygromycin (50 µg/ml for *proVAMP714::VAMP714:CFP*
176 and *proVAMP714::VAMP714:mCherry*).
177 Transient expression of *pro35S*::*VAMP714::GFP* and *ST–RFP* constructs was
178 carried out in onion epidermal peels following microprojectile bombardment using the
179 Helios Gene Gun system (Bio-Rad Laboratories, Hemel Hempstead, UK). Plates
180 containing bombarded onion sections were covered with aluminium foil and incubated at
181 22^0 C overnight, after which the inner layer of the onion tissue was peeled off carefully and
182 mounted on a glass slide with drop of water, covered with a coverslip and viewed under a
183 Leica SP5 Laser Scanning Microscope (Leica Instruments, Heidelberg, Germany).
184
185 *Gene expression analysis*
186 Localization of GUS enzyme activity in transgenic plants containing the
187 *proVAMP714::GUS* reporter gene was performed as described (Short *et al*., 2018). Stained
188 samples were fixed in Karnovsky's fixative (4% paraformaldehyde and 4% (v/v)
189 glutaraldehyde in 0.1 M phosphate buffer), dehydrated in an ethanol series and embedded
190 in LR White resin (Historesin™ Embedding Kit, Leica Instruments, Heidelberg, Germany)
191 prior to sectioning, as described (Topping *et al*., 1997).
192 For transcript analysis, RNA was extracted from seedlings 7 dpg using the
193 RNeasy Plant RNA Extraction kit (Qiagen Ltd., Surrey, UK). RT-PCR was performed

194 using the OneStep RT-PCR kit (Qiagen) as per the manufacturer's instructions.
195 Oligonucleotide primer pairs used for amplification of *VAMP714* were: 5'-
196 GTCGAGCAGAGATCCTAGTTAGTGAGTCC-3' and 5'-
197 GTCGAGGTGATTCGATGACAGAGAGTGGAG-3' primers. The *ACTIN2* gene was
198 used as a positive control, using primers 5'-GGATCGGTGGTTCCATTCTTGC-3' and 5'-
199 AGAGTTTGTCACACACAAGTGCA-3'.
200 For quantitative RT-PCR, the following primers were used: for *VAMP714*, 5'-
201 GAGATTCGATCGGTCATGGT-3' and 5'-GGTAAAGTGATTCCTCCG-3'; for
202 *VAMP713*, 5'-TTGTGAAAACATATGGCCGA-3' and 5'-
203 CTAGCAACTCCAAACGCTCC-3'; for *VAMP712*, 5'-AACGTACTGATGGCCTCACC-
204 3' and 5'-ATGTTCGCGGTTTTATCGAC-3'; for *VAMP711*, 5'-
205 GGTGGAGAAACTGCAAGCTC-3' and 5'-ACACACTTCGCAAAGCAATG-3'; for
206 *IAA1*, 5'-GGAAGTCACCAATGGGCTTA-3' and 5'-GAGATATGGAGCTCCGTCCA-
207 3'; and for *IAA2*, 5'-CACCAGTGAGATCTTCCCGT-3' and 5'-
208 AGTCTAGAGCAGGAGCGTCG-3'.
209
210 *Auxin transport assays*
211 Basipetal shoot auxin transport assays were carried out as described (Chilley *et al*., 2006).
212 2.5 cm of inflorescence stem segments lacking branches were excised and the apical
213 (upper) end placed in 20 µl MS salts medium in Eppendorf tubes. This pre-treatment
214 prevents air bubbles entering the auxin transport system. Stem segments were then
215 transferred to fresh tubes containing medium supplemented with 0.08 µCi/ml ^{3}H-IAA
216 (approx 3.5 µM IAA), again with the apical ends in the liquid medium. Samples were
217 incubated for 18 hours before the basal 5 mm of the sample was removed and placed in 4
218 ml of scintillation fluid, and incubated for 48 hours before scintillation. Non-inverted
219 samples (in which the basal ends were placed in the medium) were included to control for
220 non-specific transport. Samples incubated in non-radioactive medium were used to detect
221 baseline activity or radioactive contamination.
222 Acropetal root auxin transport assays were carried out on 2 dpg Arabidopsis
223 seedlings. Agar blocks (1 % w/v, 2-3 mm wide) were prepared containing 500 nM ^{3}H-IAA
224 (specific activity is 5.75 µCi/ml; GE Amersham UK) plus 10 µM IAA in 1% v/v DMSO.
225 The ^{3}H-IAA blocks were placed onto the top of roots just below the root-shoot junction.
226 For each root analysed, the distance between the application site and the root tip was
227 constant; the plants were inverted and left for 1 hour per cm. The distal 5 mm at the root

228 tip was removed and the sample transferred to 4 ml scintillation fluid (EcoScint A, National
229 Diagnostics) and incubated for 48 hours before measuring in the scintillation counter.
230 All data were expressed as distintegrations per minute (DPM). Results represent
231 the means of five independent assays ± SD.
232
233 *Protein localization and confocal microscopy*
234 PIN protein immunolocalization was carried out as described (Short *et al*., 2018).
235 Fluorescence levels were quantified using ImageJ software (National Institutes of Health,
236 http://rsb.info.nih.gov/ij). At least three independent analyses were carried out, and for
237 each, six random samples for each of 10 roots were measured, using identical confocal
238 settings for each analysis. Results are presented as means ± standard deviation. We thank
239 Prof. Klaus Palme (University of Freiburg) for kindly donating PIN antibodies. Confocal
240 imaging used a Leica SP5 Laser Scanning Microscope (Leica, Heidelberg, Germany).
241 Light microscopy used a Zeiss Axioscop microscope (Carl Zeiss Ltd, Welwyn Garden City,
242 UK) with DIC/Nomarski optics or an Olympus SZH10 microscope system (Olympus
243 Microscopes, Southend-on-Sea, UK).
244
245 **Results**
246 We used an activation tagging screen (Casson & Lindsey, 2006) to identify Arabidopsis
247 mutants defective in root development, and one was associated with the upregulation of
248 gene At5g22360, encoding the 221 amino acids VAMP714 protein - this gene was then the
249 focus of further studies (Fig. 1a). To confirm a potential role of the *VAMP714* gene in root
250 development, two independent loss-of-function insertional mutants were identified from
251 the SALK and GABI-Kat collections of T-DNA insertion mutants (SALK_005917 and
252 GABI_844B05; www.signal.salk.edu), and a dominant negative mutant was constructed
253 (Fig. S1). PCR-based genotyping was used to confirm the sites of T-DNA insertion in the
254 SALK and GABI-Kat lines. In the SALK mutant the T-DNA was located in the first intron,
255 and in the GABI-Kat mutant the T-DNA was located in the third exon. The dominant
256 negative gene construct was designed to comprise the Longin and SNARE domains but
257 lack the transmembrane domain, so that it would bind to the Qa, Qb and Qc complex of
258 SNARE but inhibit the binding of the native protein (Tyrrell *et al*., 2007; Fig. S1).
259 Seedlings of both *vamp714* mutants each showed very similar phenotypes, and
260 were smaller than wildtype, with reduced root systems (Figs. 1b,c). The mutant phenotype
261 was functionally complemented by a *proVAMP714::VAMP714:mCherry* transgene (Fig.

262 1c), showing that the correct gene had been identified, corresponding to the phenotype. By
263 21 dpg *vamp714* insertional mutants grown in soil developed a shorter primary root than
264 wildtype (1.2 ± 0.2 cm versus 3.5 ± 0.5 cm, n = 20; Fig. 2a), with fewer lateral roots (3.1
265 ± 1.0 versus 10.0 ± 2.0, n = 20; Fig. 2b) though this represents only a slightly reduced
266 lateral root density (a mean of 2.6 lateral roots per cm at 21 dpg for *vamp714* compared
267 with 2.8 for wildtype). Both transgenic *VAMP714* overexpressers (Fig. 1d) and dominant-
268 negative mutants also showed a reduced root system (Fig. 1e), with a mean primary root
269 length of 1.8 ± 0.2 cm (n = 20) at 21 dpg, and mean lateral root numbers of 3.2 ± 0.9, n =
270 20. Compared to wildtype, the transgenic overexpressors, *vamp714* loss-of-function
271 mutants and dominant negative mutant plants each showed a dwarfed and excessive leaf
272 and shoot branching phenotype (Fig. 2c-f). As seen in other systems, the phenotypic
273 similarities between plants with loss-of-function and gain-of-function (over-/mis-
274 expressors) of VAMP714 may be due to the disruption of interaction with partner proteins
275 in both mutants and over-/misexpressors (reviewed by Prelich, 2012), and this observation
276 suggests that the stoichiometry of protein complexes in which VAMP714 in involved is
277 required for correct function.

278 Propidium iodide staining of *vamp714* mutant roots reveals a more disorganized
279 tissue patterning compared with Col-0 (Fig. 3a-d). Lugol staining of *vamp714* mutant roots
280 similarly showed an abnormal patterning of starch grain-containing columella cells,
281 lacking both the discrete columella tier delineation seen in the wildtype and specification
282 of the quiescent centre (QC) - *vamp714* mutants lack an appropriately specified QC and
283 the columella stem cells showed evidence of differentiation (starch accumulation),
284 suggesting a failure of QC activity (Fig. 3e-h). To further investigate QC and stem cell
285 gene expression in these plants, we measured the transcription of the genes *SHORTROOT*
286 (*SHR*) and *SCARECROW* (*SCR*) (Sabatini *et al*., 2002) at 7 dpg by qRT-PCR. The
287 transcript levels of both genes were reduced in *vamp714* insertional mutants, dominant
288 negative mutants and overexpressers, consistent with the loss of identity of QC cells and
289 possibly of other stem cells in which these genes are expressed (Fig. 3i).

290 Consistent with the predicted role as a vesicle-associated membrane protein, a
291 VAMP714:GFP fusion (under the transcriptional control of the *CaMV35S* gene promoter)
292 was constructed for testing *in vivo*, and found to locate to vesicles. Given that a
293 VAMP714:mCherry fusion protein is functional, as demonstrated by genetic
294 complementation (Fig. 1c), we expect a VAMP714:GFP fusion to similarly be functional.
295 Stably transformed Arabidopsis plants expressing *pro35S::VAMP714:GFP*, and

296 transiently transformed onion epidermal peels or tobacco leaf, show GFP signal in discrete
297 vesicles, with additional plasma membrane localization seen in the stable transformants
298 (Fig. 4). The vesicles were identified as Golgi by co-labelling with the Golgi membrane
299 marker ST–RFP (sialyltransferase–red fluorescent protein, Runions *et al*., 2006; Fig. 4a-d)
300 and also some co-localization with the endoplasmic reticulum-targeted red fluorescent
301 protein RFP-HDEL (Lee *et al*., 2013; Fig. 4e-g) and at the plasmamenbrane (Fig. 4h). This
302 is consistent with computational and previous experimental predictions of subcellular
303 location in Arabidopsis (Uemura *et al*., 2004; Fig. 4i). We showed by video confocal
304 microscopy that the vesicles are mobile (Fig. 4h and Video S1).

305 The spatial expression pattern of the *VAMP714* gene was examined in seedlings
306 expressing a promoter reporter fusion (*proVAMP714*::*GUS)* using histochemical
307 localization of GUS activity (nine independent transgenic lines showed similar patterns of
308 GUS activity; representative images are shown in Fig. S2a-e). GUS activity was detected
309 in roots, and most strongly in vascular tissues of primary and lateral roots, though also at
310 lower levels in the root cortex and in the QC; and at relatively low levels in cotyledon veins,
311 but not in leaf. This expression pattern is consistent with data from the analysis of the
312 transcriptomes of individual root cell types in day 6 seedlings (Birnbaum *et al*., 2003; Nawy
313 *et al*., 2003; and visualized at www.bar.utoronto.ca; Fig. S2f).

314 Since primary and lateral root growth, correct columella patterning, and shoot
315 branching control are dependent on correct auxin transport and/or signal transduction, and
316 *VAMP714* is expressed in roots and vascular tissues that have relatively high auxin
317 responses (Perret *et al*., 2009; Sabatini *et al*., 1999), these observations led us to
318 hypothesize a role for *VAMP714* in auxin signalling.

319 To investigate auxin responses in mutant and overexpressing plants, we measured
320 the transcription of the auxin-regulated genes *IAA1* and *IAA2* (Hagen & Guilfoyle, 2002)
321 at 7 dpg by qRT-PCR. The transcript levels of both genes were found to be reduced
322 compared to wildtype in *vamp714* insertional mutants, dominant negative mutants and also
323 in *VAMP714* overexpressors (Fig. 5a). Histochemical analysis of the auxin reporter genes
324 *IAA2::GUS* (Swarup *et al*., 2001) and *DR5::GFP* (Sabatini *et al*., 1999) revealed altered
325 expression patterns in the *vamp714* mutants and overexpressor (Fig. 5b,c). Compared to
326 wildtype, *IAA2::GUS* staining is distally shifted to the disorganized columella of both
327 *vamp714* mutant and overexpressing seedlings (Fig. 5b); while *DR5::GFP*, which is
328 mainly detected in the quiescent centre and columella in the wildtype, exhibits a broadly
329 similar spatial pattern in the roots of the mutants and overexpressers to wildtype but reveals

330 the disorganized cellular patterning of the mutants and overexpressers (Fig. 5c). These
331 data are indicative of incorrect auxin distribution or auxin content in the root tip and
332 demonstrate that wildtype *VAMP714* expression is required for correct auxin distribution
333 and responses. Gravitropism is an auxin-mediated response and linked to correct function
334 of starch-containing columella cells (Wolverton *et al*., 2011), and in gravitropism assays,
335 only 10% of *vamp714* roots showed a true gravitropic response, compared to 85% of
336 wildtype roots at 24 h (n = 20; Fig. 5d,e). This further supports a role for VAMP714 in
337 auxin-mediated processes.

338 Given that VAMP714 is required for correct auxin patterning and responses, we
339 considered that it might itself be activated in response to auxin, since for example auxin
340 promotes *PIN* gene expression and PIN protein localization (Paciorek *et al*., 2005; Heisler
341 *et al*., 2005). To investigate this hypothesis, wildtype seedlings were transferred to medium
342 containing 10 µM IAA and the steady state transcript levels of *VAMP714* were measured
343 after 12, 24 and 36 h. The auxin treatment increased relative transcript abundance for the
344 *VAMP714* gene ca. 3 fold by 24 h after treatment, compared to an *ACTIN2* internal control
345 gene (Fig. 6a).

346 To study the dependence of *VAMP714* expression on correct auxin transport and
347 signalling *in planta*, we compared *VAMP714* expression in *pin1* and *aux1* mutants with
348 wildtype. The *pin1* and *aux1* mutants exhibit reduced polar auxin transport (Okada *et al*.,
349 1991; Bennett *et al*., 1996). In both mutants, the level of *VAMP714* mRNA was
350 significantly reduced compared to wildtype (Fig. 6b).

351 While exogenous cytokinin and ACC had no detectable effect on
352 *proVAMP714*::*GUS* expression (data not shown), exogenous auxin (10 µM IAA) induced
353 strong GUS activity in root tips (Fig. 6c,d), and in cotyledon vascular tissues (Fig. 6e,f).
354 10 µM TIBA treatment, which induces the accumulation of auxin in aerial tissues by
355 inhibition of polar auxin transport, led to an activation of GUS activity in the young leaf
356 (Fig. 6g,h). Consistent with its auxin inducibility, sequence analysis of a 2 kb promoter
357 region upstream of the *VAMP714* gene revealed the presence of an auxin-response element
358 (AuxRE) motif (TGTCTC) (Sabatini *et al*., 1996) at position -1346, though the
359 functionality of this element was not tested experimentally. The observed auxin-
360 inducibility of expression is consistent with *VAMP714* transcription in vascular and QC
361 cells, which contain relatively high concentrations of auxin (Sabatini *et al*., 1996; Dengler,
362 2001).

363 In view of the diverse auxin signalling-related defects in *vamp714* mutants and
364 overexpressers, and the prospective role for VAMP714 in membrane vesicles, we
365 investigated a possible role for VAMP714 in PIN localization and polar auxin transport. In
366 wildtype cells, PIN1:GFP was localized as expected to the basal membrane of the cells in
367 the central cylinder (Fig. 7a), and PIN2:GFP was localized to the apical membrane of the
368 cells in the root cortex and epidermis (Fig. 7b), as expected. Both PIN1 and PIN2 were less
369 concentrated at the plasmamembrane in mutant, dominant negative and overexpressing
370 plants (Fig. 7c). The reduction of PIN localisation at the plasmamembrane was
371 accompanied by higher protein levels in the cytoplasm, resulting in lower values of
372 membrane:cytoplasm ratios of PIN1 and PIN2 in the null mutant (Fig. 7d). In transgenic
373 plants expressing *proVAMP714::VAMP714:CFP*, both PIN1:GFP and VAMP714:CFP,
374 and PIN2:GFP and VAMP714:CFP, co-localize at the plasmamembrane, though less
375 clearly for PIN2 than for PIN1 (Fig. 7a,b). This may be linked to the stronger expression
376 of the *VAMP714* gene in vascular tissues, where PIN1 is strongly expressed, while PIN2 is
377 localized to epidermal and cortical cell layers.
378 To examine the effect of aberrant PIN localisation on auxin transport, we used a
379 [^{3}H]-IAA transport assay. The rate of auxin transport was significantly reduced in both
380 hypocotyl (Fig. 7e) and root (Fig. 7f) of the PIN localization-defective *VAMP714*
381 misexpressors, compared with wildtype controls. Given the proposed regulatory loop in
382 which auxin promotes *PIN* gene expression which then regulates directional auxin
383 transport (Grieneisen *et al*., 2007), we hypothesized that the levels of *PIN* gene expression
384 in the loss-of-function *vamp714* might also be reduced. Consistent with this hypothesis,
385 the transcription of *PIN1*, *PIN2* and *PIN4* genes was reduced in the *vamp714* loss-of-
386 function mutant (Fig. 7g).
387 The PIN proteins are dynamically regulated in their subcellular localization via
388 the endsome recycling pathway (Geldner *et al*., 2001), and we hypothesized that
389 VAMP714-associated vesicles may also be subject to endosome recycling. This recycling
390 is inhibited by both the vesicle-trafficking inhibitor brefeldin A (BFA), leading to the
391 intracellular accumulation of BFA bodies, and by the actin depolymerizing agent
392 latrunculin B (LatB) (Geldner *et al*., 2001). To determine whether VAMP714 is also
393 subject to actin-dependent endosome recycling, we treated
394 *proVAMP714::VAMP714:mCherry* seedlings with 50 μM BFA or 20 μM LatB, and
395 monitored the formation of VAMP-positive BFA bodies in root cells. We also treated
396 *proPIN1::PIN1:GFP* and *proPIN2::PIN2:GFP* seedlings with 50 μM BFA as positive

397 controls. The VAMP714:mCherry fusion protein was demonstrated to be biologically
398 functional, as shown by transgenic complementation of the *vamp714* loss-of-function
399 mutant (Fig. 1c). We found that VAMP714, PIN1 and PIN2 exhibit the same BFA body
400 formation, which can be washed out (Fig. 8a), indicative of endosome recycling between
401 BFA compartments and the plasma membrane. We also found that LatB caused
402 intracellular accumulation of VAMP714 vesicles (Fig. 8b). This suggests that VAMP714
403 forms part of both the exocytic vesicle trafficking pathway from the ER/Golgi and the
404 actin-dependent endocytic recycling pathway, which together regulate PIN protein
405 concentrations at the plasma membrane. Relatively high intracellular levels of both
406 PIN1:GFP and PIN2:GFP, and some intracellular PIN1:GFP-positive vesicle-like
407 structures are seen in the *vamp714* mutant, DN and overexpressers compared with wildtype
408 (Fig. 8c), broadly consistent with the observations for PIN immunolocalization (Fig. 7c)
409 and indicative of a requirement of VAMP714 for polar PIN localization.
410 We therefore also investigated the role of VAMP714 in endocytic recycling. We
411 monitored PIN1 and PIN2 recycling in the *vamp714* loss-of-function and dominant
412 negative mutants in the presence of 50 μM BFA. We found that PIN accumulation in BFA
413 bodies does not occur in either mutant background (Fig. 8c). This suggests that VAMP714
414 is required for PIN endosome recycling.
415
416 **Discussion**
417 Auxin homeostasis, transport and signalling each play major roles in multiple
418 developmental pathways in plants, and directional transport is key to establishing
419 functional concentration gradients of auxin that mediate the control of cell identity, tropic
420 growth and the nature of interactions with other hormones to elicit specific responses
421 (Benjamins & Scheres, 2008). Directional transport of auxin is principally mediated by
422 PIN protein family members, some of which become localized to specific faces of the cell
423 plasma membrane; and expression of *PIN* genes appears to reflect local auxin
424 concentrations, reflective of a feedback regulatory system (Omelyanchuk *et al*., 2016). PIN
425 localization involves an actin-mediated recyling between the plasma membrane and
426 endosomes, providing a mechanism for rapid changes in the placement of these
427 transporters. It is now well established that ARF GEF- and Rab5 GTPase-dependent
428 recycling is critical for PIN localization, and this process is itself inhibited by BFA (an
429 ARF GEF inhibitor) and modulated by auxin (Steinmann *et al*., 1999; Geldner *et al*., 2001;
430 Kleine-Vehn *et al*., 2008; Kitakura *et al*., 2011). Less clear have been the mechanisms

431 regulating the exocytic delivery of PIN proteins from the ER/Golgi to the plasma
432 membrane. We show in this paper that the Arabidopsis R-SNARE VAMP714 is required
433 for correct PIN localization, likely via both the exocytic and endosome recycling pathways.
434 SNAREs have been classified as vesicle-associated (v-SNAREs) and target
435 membrane-associated SNAREs (t-SNAREs) (Sollner *et al*., 1993), though under a
436 structural classification they can be grouped as Q- and R-SNAREs, owing to the occurrence
437 of either a conserved glutamine or arginine residue in the centre of the SNARE domain
438 (Fasshauer *et al*., 1998). Generally, t-SNAREs correspond to Q-SNAREs, and v-SNAREs
439 correspond to R-SNAREs. There are more than 60 SNARE protein-encoding genes
440 represented in the Arabidopsis genome (Uemura *et al*., 2004; Lipka *et al*., 2007; Sanderfoot,
441 2007), but there is limited information available on the roles of SNARE proteins from
442 genetic studies in plants, most likely because of a lack of loss-of-function phenotypes due
443 to functional redundancy between related family members. For example, redundancy has
444 been demonstrated between VTI11 and VTI12 (Kato *et al*., 2002; Surpin *et al*., 2003),
445 SYP121 and SYP122 (Assaad *et al*., 2004; Zhang *et al*., 2008), and VAMP721 and
446 VAMP722 (Kwon *et al*., 2008).
447 The animal VAMP synaptobrevin has been implicated in linking synaptic vesicles
448 to the plasma membrane (Walch-Solimena *et al*., 1993; Bonifacino & Glick, 2004). It is
449 proposed that R-SNAREs may play a key role in determining specificity in vesicle budding,
450 and an important mechanism for SNARE localization is interaction with vesicle coats. For
451 example, it has been shown that R-SNAREs may be components of the COPII vesicles that
452 are involved in ER-Golgi transport (Springer & Schekman, 1998), and that R-SNAREs
453 must be packaged into COPI vesicles during retrieval from the Golgi (Rein *et al*., 2002).
454 The data presented in this paper provides new information on both the role of the
455 R-SNARE VAMP714 and the molecular components required for the control of auxin
456 transport and auxin-mediated responses via PIN protein expression, recycling and
457 localization. We propose a model in which the correct delivery of PIN proteins from the
458 ER/Golgi to the plasma membrane is via a VAMP714-associated compartment, that is a
459 necessary precursor to the endocytic recycling that provides dynamical control over the
460 level and site of PIN protein localization (Fig. S3). This in turn regulates the direction and
461 rate of auxin efflux. We show that VAMP714 is required for a range of correct auxin
462 responses, including auxin-mediated gene expression, root gravitropism, root cell
463 patterning and shoot branching.

464 This model is supported by the co-localization of VAMP714 and PIN proteins at
465 the plasma membrane; the accumulation of PIN proteins in the cytoplasm in *vamp714* loss-
466 of-function and dominant negative mutants and VAMP714 misexpressers; and the
467 requirement for wildtype levels of expression of *VAMP714* for BFA body formation (i.e.
468 endosome recycling). Significantly, SNARES and Rab GTPases have been demonstrated
469 to interact functionally to promote vesicle fusion at the endosome, and act coordinately to
470 increase the specificity and efficiency of membrane fusion (Ohya *et al*., 2009; Ebine *et al*.,
471 2011). Mechanistically VAMP714 may interact with the RAB5 GTPase complex known
472 to participate in PIN recycling at the endosome (Dhonukshe *et al*., 2008), following its
473 exocytic transport of PINs, and this possibility is the subject of further studies. It is also
474 currently unclear whether VAMP714 is involved in transcytosis to modulate PIN
475 localization; and whether it is required for PIN-specific or more general transport of plasma
476 membrane proteins.
477 In the classical canalization hypothesis pioneered by Sachs (Sachs, 1981), auxin
478 itself promotes its own transport system, leading to directional flow through tissues and
479 subsequent establishment of cell polarity and differentiation. Consistent with this
480 hypothesis, the auxin-mediated transcriptional activation of the *VAMP714* gene would
481 allow the activation of a pathway essential for polar auxin transport by promoting correct
482 PIN protein localization at the plasma membrane. Integrated in this mechanism would be
483 auxin-mediated transcriptional effects on *PIN* genes (Heisler *et al*., 2005) and the effect of
484 auxin on PIN endocytosis (Paciorek *et al*., 2005). A role for VAMP714 in the (probably
485 indirect) maintenance of *PIN* gene expression is also indicated. Our studies demonstrate
486 that R-SNARE-dependent exocytosis is essential for the auxin transport and downstream
487 signalling pathways that are required for the control of cell polarity, tropic growth and
488 morphogenesis in plants.
489

490 **Acknowledgements**
491 KL acknowledges The Biotechnology and Biological Sciences Research Council
492 (BBS/B/0773X) and Durham University for funding. XG thanks the China Scholarship
493 Council for funding to support her studies at Durham University.
494

495 **Author contributions**

496 KL, SAC and JFT devised the project; XG, KF and SAC carried out the experimental work;
497 KL, JFT, PJH and GG supervised the work; KL drafted the manuscript; all authors edited
498 the manuscript.
499
500 **Data availability statement**
501 All materials and data described in this papaer are available to readers from the
502 corresponding author, upon reasonable request.
503
504 **References**

505 **Assaad FF, Qiu JL, Youngs H, Ehrhardt D, Zimmerli L, Kalde M, Wanner G, Peck**
506 **SC, Edwards H, Ramonell K, Somerville CR, Thordal-Christensen H. 2004.** The
507 PEN1 syntaxin defines a novel cellular compartment upon fungal attack and is required
508 for the timely assembly of papillae. *Molecular Biology of the Cell* **15**: 5118-5129.
509 **Benjamins R, Scheres B. 2008.** Auxin: the looping star in plant development. *Annual*
510 *Review of Plant Biology* **59**: 443-465.
511 **Bennett MJ, Marchant A, Green HG, May ST, Ward SP, Millner PA, Walker AR,**
512 **Schulz B, Feldmann KA. 1996.** Arabidopsis *AUX1* gene: a permease-like regulator of
513 root gravitropism. *Science* **273**: 948-950.
514 **Birnbaum K, Shasha DE, Wang JY, Jung JW, Lambert GM, Galbraith DW, Benfey**
515 **PN. 2003.** A gene expression map of the Arabidopsis root. *Science* **302**: 1956-1960.
516 **Bonifacino JS, Glick, BS. 2004.** The mechanisms of vesicle budding and fusion. *Cell* **116**:
517 153-166.
518 **Brand U, Fletcher JC, Hobe M, Meyerowitz EM, Simon R. 2000.** Dependence of stem
519 cell fate in Arabidopsis on a feedback loop regulated by CLV3 activity. *Science* **289**:
520 617-619.
521 **Casson SA, Lindsey K. 2006.** The *turnip* mutant of Arabidopsis reveals that *LEC1*
522 expression mediates the effects of auxin and sugars to promote embryonic cell identity.
523 *Plant Physiology* **142**: 526-541.
524 **Casson SA, Topping JF, Lindsey K. 2009.** MERISTEM-DEFECTIVE, an RS domain
525 protein, is required for meristem patterning and function in Arabidopsis. *Plant Journal*
526 **57**: 857-869.
527 **Chilley PM, Casson SA, Tarkowski P, Wang KLC, Hawkins N, Hussey PJ, Beale M,**
528 **Ecker JR, Sandberg GK, Lindsey K. 2006.** The POLARIS peptide of Arabidopsis

529 regulates auxin transport and root growth via effects on ethylene signalling. *Plant Cell*
530 **18**: 3058-3072.
531 **Collins NC, Thordal-Christensen H, Lipka V, Bau S, Kombrink E, Qiu JL,**
532 **Huckelhoven R, Stein M, Freialdenhoven A, Somerville SC, Schulze-Lefert, P.**
533 **2003.** SNARE-protein-mediated disease resistance at the plant cell wall. *Nature* **425**:
534 973-977.
535 **Clough SJ, Bent AF. 1998.** Floral dip: a simplified method for Agrobacterium-mediated
536 transformation of *Arabidopsis thaliana*. *Plant Journal* **6**: 735-743.
537 **Dacks JB, Doolittle WF. 2002.** Novel syntaxin gene sequences from Giardia,
538 Trypanosoma and algae: implications for the ancient evolution of the eukaryotic
539 endomembrane system. *Journal of Cell Science* **115**: 1635-1642.
540 **Dale PJ, Marks MS, Brown MM, Woolston CJ, Gunn HV, Mullineaux P, Lewis DM,**
541 **Kemp JM, Chen, DF. 1989.** Agroinfection of wheat-inoculation of in vitro grown
542 seedlings and embryos. *Plant Science* **63**: 237-245.
543 **Dengler, N. G. 2001.** Regulation of vascular development. *Journal of Plant Growth*
544 *Regulation* **20**: 1-13.
545 **Dhonukshe P, Tanaka H, Goh T, Ebine K, Mahonen AP, Prasad K, Blilou I, Geldner**
546 **N, Xu J, Uemura T, Chory J, Ueda T, Nakano A, Scheres B, Friml J. 2008.**
547 Generation of cell polarity in plants links endocytosis, auxin distribution and cell fate
548 decisions. *Nature* **456**: 962-967.
549 **Ebine K, Fujimoto M, Okatani Y, Nishiyama T, Goh T, Ito E, Dainobu T, Nishitani**
550 **A, Uemura T. Sato MH, Thordal-Christensen H, Tsutsumi N, Nakano A, Ueda, T.**
551 **2011.** A membrane trafficking pathway regulated by the plant-specific RAB GTPase
552 ARA6. *Nature Cell Biology* **13**: 853-860.
553 **EI-Kasmi F, Krause C, Hiller U, Stierhof YD, Mayer U, Conner L, Kong**
554 **LT, Reichardt I, Sanderfoot AA, Jürgens G. 2013.** SNARE complexes of different
555 composition jointly mediate membrane fusion in Arabidopsis cytokinesis. *Molecular*
556 *Biology of the Cell* **24**: 1505-1613.
557 **Enami K, Ichikawa M, Uemura T, Kutsuna N, Hasezawa S, Nakagawa T, Nakano A,**
558 **Sato MH. 2009.** Differential expression control and polarized distribution of plasma
559 membrane-resident SYP1 SNAREs in *Arabidopsis thaliana*. *Plant and Cell Physiology*
560 **50**: 280-289.

561 **Fasshauer D, Sutton RB, Brunger AT, Jahn R. 1998.** Conserved structural features of
562 the synaptic fusion complex: SNARE proteins reclassified as Q- and R-SNAREs.
563 *Proceedings of the National Academy of Sciences USA* **95**: 15781-15786.
564 **Geldner N, Friml J, Stierhof YD, Jürgens G, Palme K. 2001.** Auxin transport inhibitors
565 block PIN1 cycling and vesicle trafficking. *Nature* **413**: 425-428.
566 **Grieneisen VA, Xu J, Maree AFM, Hogeweg P, Scheres B. 2007.** Auxin transport is
567 sufficient to generate a maximum and gradient guiding root growth. *Nature* **449**: 1008-
568 1013.
569 **Hagen G, Guilfoyle TJ. 2002.** Auxin-responsive gene expression: genes, promoters and
570 regulatory factors. *Plant Molecular Biology* **49**: 373-385.
571 **Heisler MG, Ohno C, Das P, Sieber P, Reddy GV, Long JA, Meyerowitz EM. 2005.**
572 Patterns of auxin transport and gene expression during primordium development
573 revealed by live imaging of the Arabidopsis inflorescence meristem. *Current Biology*
574 **15**: 1899-1911.
575 **Hong W. 2005.** SNAREs and traffic. *Biochimica Biophysica Acta* **1744**: 120-144.
576 **Karnik R, Grefen C, Bayne R, Honsbein A, Köhler T, Kioumourtzoglou D, Williams**
577 **M, Bryant NJ, Blatt MR. 2013.** Arabidopsis Sec1/Munc18 Protein SEC11 is a
578 competitive and dynamic modulator of SNARE binding and SYP121-dependent vesicle
579 traffic. *Plant Cell* **25**: 1368-1382.
580 **Kato T, Morita MT, Fukaki H, Yamauchi Y, Uehara M, Niihama M, Tasaka M. 2002.**
581 SGR2, a phospholipase-like protein, and ZIG/SGR4, a SNARE, are involved in the
582 shoot gravitropism of Arabidopsis. *Plant Cell* **14**: 33-46.
583 **Kitakura S, Vanneste S, Robert S, Lofke C, Teichmann T, Tanaka H, Friml J. 2011.**
584 Clathrin mediates endocytosis and polar distribution of PIN auxin transporters in
585 Arabidopsis. *Plant Cell* **23**: 1920-1931.
586 **Kleine-Vehn J, Dhonukshe P, Sauer M, Brewer P, Wisniewska J, Paciorek T,**
587 **Benkova E, Friml J. 2008.** ARF GEF-dependent transcytosis and polar delivery of PIN
588 auxin carriers in Arabidopsis. *Current Biol*ogy **18**: 526-531.
589 **Kwon C, Neu C, Pajonk S, Yun HS, Lipka U, Humphry M, Bau S, Straus M,**
590 **Kwaaitaal M, Rampelt H, El Kasmi F, Jürgens G, Parker J, Panstruga R, Lipka**
591 **V, Schulze-Lefert P. 2008.** Co-option of a default secretory pathway for plant immune
592 responses. *Nature* **451**: 835-840.
593 **Laux T, Mayer KF, Berger J, Jürgens G. 1996.** The *WUSCHEL* gene is required for
594 shoot and floral meristem integrity in Arabidopsis. *Development* **122**: 87-96.

595 **Lee H, Sparkes I, Gattolin S, Dzimitrowicz N, Roberts LM, Hawes C, Frigerio L. 2013.**
596 An Arabidopsis reticulon and the atlastin homologue *RHD3-like2* act together in shaping
597 the tubular endoplasmic reticulum. *New Phytologist* **197**: 481-489.
598 **Leshem Y, Golani Y, Kaye Y, Levine A. 2010.** Reduced expression of the v-SNAREs
599 AtVAMP71/AtVAMP7C gene family in Arabidopsis reduces drought tolerance by
600 suppression of abscisic acid-dependent stomatal closure. *Journal of Experimental*
601 *Botany* **61**: 2615-2622.
602 **Leshem Y, Melamed-Book N, Cagnac O, Ronen G, Nishri Y, Solomon M, Cohen G,**
603 **Levine A. 2006.** Suppression of Arabidopsis vesicle-SNARE expression inhibited
604 fusion of H_2O_2 containing vesicles with tonoplast and increased salt tolerance.
605 *Proceedings of the National Academy of Sciences USA* **103**: 18008-18013.
606 **Levine A, Belenghi B, Damari-Weisler H, Granot D. 2001.** Vesicle-associated
607 membrane protein of Arabidopsis suppresses Bax-induced apoptosis in yeast
608 downstream of oxidative burst. *Journal of Biological Chemistry* **276**: 46284-46289.
609 **Lipka V, Kwon C, Panstruga R. 2007.** SNARE-ware: the role of SNARE-domain
610 proteins in plant biology. *Annual Review of Cell and Developmental Biology* **23**: 147-
611 174.
612 **Nawy T, Lee JY, Colinas J, Wang JY, Thongrod SC, Malamy JE, Birnbaum K,**
613 **Benfey, PN. 2005.** Transcriptional profile of the Arabidopsis root quiescent center.
614 *Plant Cell* **17**: 1908-1925.
615 **Ohya T, Miaczynska M, Coskun U, Lommer B, Runge A, Drechsel D, Kalaidzidis Y,**
616 **Zerial M. 2009.** Reconstitution of Rab- and SNARE-dependent membrane fusion by
617 synthetic endosomes. *Nature* **459**: 1091-1097.
618 **Okada K, Ueda J, Komaki MK, Bell CJ, Shimura Y. 1991.** Requirement of the auxin
619 polar transport system in the early stages of Arabidopsis floral bud formation. *Plant Cell*
620 **3**: 677-684.
621 **Omelyanchuk NA, Kovrizhnykh VV, Oshchepkova EA, Pasternak T, Palme K,**
622 **Mironova VV. 2016.** A detailed expression map of the PIN1 auxin transporter in
623 *Arabidopsis thaliana* root. *BMC Plant Biology* **16** (suppl. 1): 5.
624 **Paciorek T, Zazimalova E, Ruthardt N, Petrásek J, Stierhof YD, Kleine-Vehn J,**
625 **Morris DA, Emans N, Jürgens G, Geldner N, Friml J. 2005.** Auxin inhibits
626 endocytosis and promotes its own efflux from cells. *Nature* **435**: 1251-1256.
627 **Peret B, Larrieu A, Bennett MJ. 2009.** Lateral root emergence: a difficult birth. *Journal*
628 *of Experimental Botany* **60**: 3637-3643.

629 **Petrášek J, Friml J. 2009.** Auxin transport routes in plant development. *Development* **136**:
630 2675-2688.
631 **Prelich G. 2012.** Gene overexpression: Uses, mechanisms and interpretation. *Genetics* **190**:
632 841-854.
633 Rein U, Andag U, Duden R, Schmitt HD, Spang A. 2002. ARF-GAP–mediated interaction
634 between the ER-Golgi v-SNAREs and the COPI coat. *Journal of Cell Biology* **157** 395-
635 404.
636 **Reinhardt D, Mandel T, Kuhlemeier C. 2000.** Auxin regulates the initiation and radial
637 position of plant lateral organs. *Plant Cell* **12**: 507-518.
638 **Runions J, Brach T, Kuhner S, Hawes C. 2006.** Photoactivation of GFP reveals protein
639 dynamics within the endoplasmic reticulum membrane. *Journal of Experimental Botany*
640 **57**: 43-50.
641 **Sabatini S, Beis D, Wolkenfelt H, Murfett J, Guilfoyle T, Malamy J, Benfey P, Leyser**
642 **O, Bechtold N, Weisbeek P, Scheres, B. 1999.** An auxin-dependent distal organizer of
643 pattern and polarity in the Arabidopsis root. *Cell* **99**: 463-472.
644 **Sabatini S, Heidstra R, Wildwater M, Scheres B. 2002.** SCARECROW is involved in
645 positioning the stem cell niche in the Arabidopsis root meristem. *Genes and*
646 *Development* **17**: 354-358.
647 **Sachs T. 1981.** The control of the patterned differentiation of vascular tissues. *Advances*
648 *in Botanical Research* **9**: 151-262.
649 **Sanderfoot AA. 2007.** Increases in the number of SNARE genes parallels the rise of
650 multicellularity among the green plants. *Plant Physiology* **144**: 6-17.
651 **Short E, Leighton, M, Imriz G, Liu D, Cope-Selby N, Hetherington F, Smertenko A,**
652 **Hussey PJ, Topping JF, Lindsey K. 2018.** Epidermal expression of a sterol
653 biosynthesis gene regulates root growth by a non-cell-autonomous mechanism in
654 *Arabidopsis*. *Development* **145**: 160572.
655 **Sollner T, Whiteheart SW, Brunner M, Erdjument-Bromage H, Geromanos S,**
656 **Tempst P, Rothman JE. 1993.** SNAP receptors implicated in vesicle targeting and
657 fusion. *Nature* **362**: 318-324.
658 **Souter M, Topping J, Pullen M, Friml J, Palme K, Hackett R, Grierson D, Lindsey**
659 **K. 2002.** *hydra* mutants of Arabidopsis are defective in sterol profiles and auxin and
660 ethylene signalling. *Plant Cell* **14**: 1017-1031.
661 **Springer S, Schekman R. 1998.** Nucleation of COPII vesicular coat complex by
662 Endoplasmic Reticulum to Golgi vesicle SNAREs. *Science* **281**: 698-700.

663 **Steinmann T, Geldner N, Grebe M, Mangold S, Jackson CL, Paris S, Gälweiler L,**
664 **Palme K, Jürgens G. 1999.** Coordinated polar localization of auxin efflux carrier PIN1
665 by GNOM ARF GEF. *Science* **286**: 316-318.
666 **Surpin M, Zheng HJ, Morita MT, Saito C, Avila E, Blakeslee JJ, Bandyopadhyay A,**
667 **Kovaleva V, Carter D, Murphy A, Tasaka M, Raikhel N. 2003.** The VTI family of
668 SNARE proteins is necessary for plant viability and mediates different protein transport
669 pathways. *Plant Cell* **15**: 2885-2899.
670 **Swarup R, Friml J, Marchant A, Ljung K, Sandberg G, Palme K, Bennett, M. 2001.**
671 Localization of the auxin permease AUX1 suggests two functionally distinct hormone
672 transport pathways operate in the Arabidopsis root apex. *Genes and Development* **15**:
673 2648-2653 (2001).
674 **Topping J, Lindsey K. 1997.** Promoter trap markers differentiate structural and positional
675 components of polar development in Arabidopsis. *Plant Cell* **9**: 1713-1725.
676 **Topping JF, May VJ, Muskett PR, Lindsey K. 1997.** Mutations in the *HYDRA1* gene of
677 Arabidopsis perturb cell shape and disrupt embryonic and seedling morphogenesis.
678 *Development* **124**: 4415-4424.
679 **Tyrrell M, Campanoni P, Sutter JU, Pratelli R, Paneque M, Sokolovski S, Blatt MR.**
680 **2007.** Selective targeting of plasma membrane and tonoplast traffic by inhibitory
681 (dominant-negative) SNARE fragments. *Plant Journal* **51**: 1099-1115.
682 **Uemura T, Nakano RT, Takagi J, Wang YM, Kramer K, Finkemeier I, Nakagami H,**
683 **Tsuda K, Ueda T, Schulze-Lefert P, Nakano A. 2019.** A Golgi-released
684 subpopulation of the trans-Golgi network mediates protein secretion in Arabidopsis.
685 *Plant Physiology* **179**: 519-532.
686 Uemura T, Ueda T, Ohniwa RL, Nakano A, Takeyasu K, Sato MH. 2004. **Systematic**
687 analysis of SNARE molecules in Arabidopsis: dissection of the post-Golgi network in
688 plant cells. *Cell Structure and Function* **29**: 49-65.
689 **Yun HS, Kwaaitaal M, Kato N, Yi C, Park S, Sato MH, Schulze-Lefert P, Kwon C.**
690 **2013.** Requirement of vesicle-associated membrane protein 721 and 722 for sustained
691 growth during immune responses in Arabidopsis. *Molecules and Cells* **35**: 481-488.
692 **Vanneste S, Friml J. 2009.** Auxin: A trigger for change in plant development. *Cell* **136**:
693 1005-1016.
694 **Vieten A, Sauer M, Brewer PB, Friml J. 2007.** Molecular and cellular aspects of auxin-
695 transport-mediated development. *Trends in Plant Science* **12**: 160-168.

696 **Walch-Solimena C, Takei K, Marek KL, Midyett K, Sudhof TC, Camilli PD, Jahn R.**
697 **1993.** Synaptotagmin: a membrane constituent of neuropeptide-containing large dense-
698 core vesicles. *Journal of Neuroscience* **13**: 3895-3903.
699 **Wiśniewska J, Xu J, Seifertova D, Brewer PB, Ruzicka K, Blilou I, Rouquie D,**
700 **Benková E, Scheres B, Friml J. 2006.** Polar PIN localization directs auxin flow in
701 plants. *Science* **312**: 883.
702 **Wolverton C, Paya AM, Toska J. 2011.** Root cap angle and gravitropic response rate are
703 uncoupled in the Arabidopsis *pgm-1* mutant. *Physiologia Plantarum* **141**: 373-382.
704 **Xue Y, Yang YQ, Yang ZJ, Wang XF, Guo Y. 2018.** VAMP711 is required for abscisic
705 acid-mediated inhibition of plasma membrane H^+-ATPase activity. *Plant Physiology*
706 **178**: 1332-1343.
707 **Yano D, Sato M, Saito C, Sato MH, Morita MT, Tasaka M. 2003.** A SNARE complex
708 containing SGR3/AtVAM3 and ZIG/VTI11 in gravity-sensing cells is important for
709 Arabidopsis shoot gravitropism. *Proceedings of the National Academy of Sciences USA*
710 **100**: 8589-8594.
711 **Zhang HY, Liu P, Hao HQ, Jin JB, Lin J. X. 2011.** Arabidopsis R-SNARE proteins
712 VAMP721 and VAMP722 are required for cell plate formation. *PLoS ONE* **6**: e26129.
713 **Zhang B, Karnik R, Wang YZ, Wallmeroth N, Blatt MR, Grefen C. 2015.** The
714 Arabidopsis R-SNARE VAMP721 interacts with KAT1 and KC1 K^+ channels to
715 moderate K^+ current at the plasma membrane. *Plant Cell* **27**: 1697-1717
716 **Zhang L, Zhao HY, Qi WC, Zheng FX, Wang TQ, Li TQ. 2017.** The analysis of mutant
717 phenotypes and tissue expression reveals a role of SNAREs VAMP721 and VAMP722
718 in seedling growth. *Biology of Plants* **61**: 275-283.
719 **Zhang Z, Lenk A, Andersson M, Gjetting T, Pedersen C, Nielsen M, Newman MA,**
720 **Houb BH, Somerville S, Thordal-Christensen H. 2008.** A lesion-mimic syntaxin
721 double mutant in Arabidopsis reveals novel complexity of pathogen defense signaling.
722 *Molecular Plant* **1**: 510-527.
723
724
725
726

727 **Figure Legends**

728

729 **Figure 1. *VAMP714* gene is required for correct seedling development.**

730 (a) Diagrammatic representation of the activation tag locus, showing the position of the
731 activation tag T-DNA and the expression analysis of the *At5g22360* and *At5g22370* genes
732 relative to the *ACTIN2* and Col-0 wild type. RB and LB indicate the borders of the T-DNA
733 insertion element, encompassing enhancer regions (the four pentagons) and showing the
734 site of insertion. The distances from the T-DNA insertion site to the transcriptional start
735 codon of each of the adjacent genes are indicated. Red asterisk indicates enhanced
736 expression of *At5g22360* (*VAMP714*) in the mutant (m), compared to in wildtype (WT).
737 (b) Wildtype (left) and activation-tagged *VAMP714* overexpressing (right) seedlings at 14
738 dpg. Bar = 5 mm.
739 (c) Seedlings (7 dpg) of wildtype (WT), *vamp714* mutant and *vamp714* mutant tranformed
740 with a *proVAM714P::VAMP&14:mCherry* gene fusion, showing functional
741 complementation of the mutant by the fusion gene. Bar = 5 mm.
742 (d) Seedlings (7 dpg) of wildtype (WT) and *pro35S::VAMP714* transgenic overexpressers.
743 Bar = 5 mm.
744 (e) Seedlings (7 dpg) of wildtype (WT) and VAMP714 dominant-negative mutant
745 transgenics. Bar = 5 mm.

746

747 **Figure 2. *VAMP714* gene is required for correct root and shoot architecture.**

748 (a) Primary root length of wildtype (WT) and *vamp714* loss-of-function mutants grown on
749 vertical agar plates over 21 dpg. Mean of 20 replicates ± standard error of the mean.
750 (b) Lateral root number of wildtype (WT) and *vamp714* loss-of-function mutants grown on
751 vertical agar plates over 21 dpg. Mean of 20 replicates ± standard error of the mean.
752 (c) Shoot phenotypes of wildtype (WT), *vamp714* mutant, VAMP714 dominant-negative
753 mutant (DN) and transgenic *VAMP714* overexpressers (VAMPOx) seedlings at 4 weeks
754 post germination. Bar = 1 cm.
755 (d) Wildtype (L) and transgenic *pro35S:VAMP714* plants (R) plants at 8 weeks post
756 germination. Bar = 3 cm.
757 (e) Rosette leaf number of wildtype (WT), *vamp714* mutant, VAMP714 dominant-negative
758 mutant (DN) and transgenic *VAMP714* overexpressers (VAMPOx) seedlings at 4 weeks
759 post germination. Error bars represent standard deviation of the mean of 3 biological
760 replicates.

761 (f) Shoot branch number of wildtype (WT), *vamp714* mutant, VAMP714 dominant-
762 negative mutant (DN) and transgenic *VAMP714* overexpressers (VAMPOx) seedlings at 8
763 weeks post germination. Error bars represent standard deviation of the mean of 3 biological
764 replicates. *** indicates significant difference at $P < 0.005$, Student's *t*-test.
765
766 **Figure 3. Functional VAMP714 is required for correct root cell patterning, QC**
767 **maintenance and meristem gene expression.**
768 (a-d) Confocal imaging of root tips of (a) wildtype (WT), (b) *vamp714* mutant, (c)
769 VAMP714 dominant negative mutant (DN) and (d) transgenic VAMP714 overexpressing
770 (vamp714Ox) seedlings (7 dpg) stained with propidium iodide. White arrows indicate
771 position of the QC cells. Bars = 10 uM.
772 (e-h) Double labeling of QC and differentiated columella cells visualized by QC25 and
773 amyloplast (lugol) staining, respectively, in wildtype (a) and mutant or overexpressing
774 seedlings (f-H) revealing defective columella stem cells (black arrows) and lack of QC
775 marker expression in *vamp714* mutant (f), VAMP714 dominant negative mutant (g) and
776 *VAMP714* transgenic overexpressing roots (h), showing defects in QC identity (red arrows)
777 and columella patterning. Bars = 10 uM.
778 (i) qRT-PCR analysis of mRNA abundance of the QC identity genes *SHR* and *SCR* in
779 wildtype (WT), *vamp714* mutants, dominant negative mutants (DN) and transgenic
780 *VAMP714* overexpressers (*vamp714Ox*), compared to *ACTIN2* expression. Data represent
781 means of 3 biological replicates ± SD. Significant differences between wildtype and mutant
782 expression at $P < 0.05$ (**) and 0.005 (***) are indicated, Student's *t*-test.
783
784 **Figure 4. VAMP714 fusion proteins localize to vesicles.**
785 (a-d) Transient expression and localization of VAMP714:GFP (a) and the Golgi membrane
786 marker ST–RFP (b), showing co-localization in merged images (c,d; arrowheads indicate
787 individual vesicles showing co-localization). Bars = 25 µm (a-c), 10 µm (d).
788 (e-g) Transient expression and localization of VAMP714:GFP (e) and the ER membrane
789 marker RFP-DEL (f), showing some co-localization in merged images (g). Bars = 15 µm
790 (h) Still image captured from a video (see Supplementary Video 1 for video sequence)
791 with temporal-color code tracking of VAMP714:mCherry-positive vesicle movement.
792 White arrows indicate the direction of vesicle transport to the plasmamembrane. Bar = 20
793 µm.

794 (i) Heat map of predicted VAMP714 subcellular location, using online tool at
795 http://bar.utoronto.ca/eplant/, showing highest levels (red) at the Golgi, ER and
796 plasmamembrane.
797
798 **Figure 5. VAMP714 is required for correct auxin-mediated gene expression and root**
799 **gravitropism.**
800 (a) qRT-PCR analysis of mRNA abundance for the auxin-inducible *IAA1* and *IAA2* genes
801 in wildtype (WT), *vamp714* mutant, VAMP714 dominant negative mutant (DN) and
802 transgenic overexpressing (VAMP Ox) seedlings at 7 dpg, compared to *ACTIN2*
803 expression.
804 (b-d) *proIAA2::GUS* reporter activity in wildtype (WT, b), *vamp714* mutant (c) and
805 transgenic overexpressing (VOX, d) roots at 7 dpg. Bars = 10 µm.
806 (e, f) *proDR5::GFP* expression in wildtype (WT), *vamp714* mutant, transgenic dominant
807 negative VAMP714 mutant (DN) and transgenic overexpressing (VAMPOx) roots at 7
808 dpg. Bars = 10 µm.
809 (d,e) Diagrammatic representation of the gravitropic responses of wildtype (d) and
810 *vamp714* mutants (e) at 24 h after shifting the vertical axis by 90°. The pie-charts indicate
811 the proportion of seedlings showing bending responses at between 80° to 90° from
812 horizontal (blue), 40° to 80° from horizontal (orange) and 20° to 40° from horizontal (grey).
813
814 **Figure 6. VAMP714 gene is auxin-regulated.**
815 (a) qRT-PCR analysis of mRNA abundance of *VAMP714* seedlings either untreated (U) or
816 treated with 100 µM IAA for 0, 12, 24 and 36 h. Expression levels are relative to *ACTIN2*
817 expression. Data represent means of 3 biological replicates ± SD.
818 (b) qRT-PCR analysis of mRNA abundance of *VAMP714* in wildtype, *pin1* and *aux1*
819 mutant seedlings at 7 dpg. Expression levels are relative to *ACTIN2* expression. Data
820 represent means of 3 biological replicates ± SD.
821 (c,d) Primary root tip of 7 dpg seedling either untreated (c) or treated with 10 µM IAA for
822 5 days (c), bars = 25 µm.
823 (e,f) Cotyledon of seedlings either untreated (e) or treated with 10 µM IAA for 5 days (f),
824 bars = 25 µm (e), 40 µm (f).
825 (g,h) Leaf of seedling either untreated (g) or treated with 10 µM TIBA for 5 days (h), bars
826 = 25 µm (g), 30 µm (h)
827

828 **Figure 7. VAMP714 is required for correct PIN protein localization and polar auxin**
829 **transport**
830 (a) proPIN1::PIN1:GFP and (b) proPIN2::PIN2:GFP localization (upper panels) and co-
831 localization with proVAMP714::VAMP714:CFP (lower two panels) at the basal
832 plasmamembrane of root vascular cells in transgenic plants. Arrowheads highlight co-
833 localization in merged images. (a) left panels: bars = 10 µm; (a) right panels: bars = 1 µm;
834 (b) bars = 10 µm.
835 (c) PIN1 and PIN2 localization in seedling roots of *vamp714* mutants (left two panels),
836 dominant negative (DN, centre two panels) and *pro35S::VAMP714* overexpressers (OX,
837 right two panels) at 7 dpg. Arrowhead exemplifies disrupted PIN localization. Bars = 20
838 µm.
839 (d) Quantification of PIN1 and PIN2 distribution in wildtype and *vamp714* mutant cells,
840 showing the proportion of cells with relatively strong fluorescence signal at the plasma
841 membrane (four-fold above the cytoplasmic signal and above; grey bars) versus relatively
842 weak signal at the plasmamembrane (less then four-fold above the cytoplasm level; black
843 bars) for wildtype (control) and mutant (*vamp714*). The mutant exhibits a lower percentage
844 of cells showing the fluoresence signal for both PIN1 and PIN2 at the plasmamembrane.
845 (e, f) Polar auxin transport measurements in (e) inflorescence stems of *vamp414* mutants
846 and (f) roots of *pro35S::VAMP714* misexpressors. (e) Col-0 indicates auxin transport in
847 the wildtype control; CNI is the non-inverted wildtype control (the stem was not inverted,
848 so that the basal region was exposed to the ^{3}H-IAA); CNR is the wildtype control in non-
849 radiactive medium; vamp indicates auxin transport in the *vamp714* mutant; vNI is the non-
850 inverted *vamp714* mutant; vNR is *vamp714* mutant incubated in non-radioactive medium.
851 Data represent the means of 5 independent assays ± SD. (f) Auxin transport assays in
852 wildtype (wt) and transgenic *pro35S::VAMP714*-overexpressing (VAMP Ox) roots. Data
853 represent the means of 5 independent assays ± SD.
854 (g) qRT-PCR analysis of mRNA abundance of *PIN1, PIN2* and *PIN4* genes in wildtype
855 (WT) and *vamp714* mutant seedlings, relative to *ACTIN2* expression. Error bars represent
856 means ± SD of 3 biological replicates.
857
858 **Figure 8. VAMP714, PIN1 and PIN2 exhibit same endosome recycling from BFA**
859 **compartments to plasma membrane and actin requirements for polar VAMP714**
860 **targeting.**

861 (a) Seedling roots expressing proPIN1::PIN1:GFP, proPIN2::PIN2:GFP and
862 proVAMP714::VAMP714:mCherry were imaged before and after 2 h of treatment with 50
863 μM brefeldin A (BFA), 30 and 90 min after BFA washout, and after a prolonged 12 h
864 treatment with BFA. The localization of PIN:GFP proteins and VAMP714:mCherry
865 proteins in the plasma membrane was re-established by 30 min after washout in the wild
866 type. Arrows indicate BFA bodies. Bars = 10 μm.
867 (b) Seedlings expressing proVAMP714::VAMP714:mCherry were imaged before and
868 after 3 h of treatment with 20 μM latrunculin B, revealing sensitivity to actin
869 depolymerization. Arrow indicates intracellular vesicle accumulation. Bars = 10 μm.
870 (c) wildtype (WT), *vamp714* mutant, and VAMP714 dominant negative mutant (DN)
871 seedlings expressing either proPIN1::PIN1:GFP or proPIN2::PIN2:GFP imaged before
872 treatment with 50 μM brefeldin A (BFA; untreated, left panels) and after 2 h of BFA
873 treatment (right panels). WT seedlings exhibited PIN:GFP internalization in BFA
874 compartments, whereas *vamp714* mutant and dominant negative mutant seedlings showed
875 no PIN accumulation in BFA bodies. Arrows indicate intracellular accumulation of PIN.
876 Bars = 10 μm.
877
878
879 **Supporting Information**
880
881 **Figure S1. Construction and analysis of dominant negative VAMP714 plants.**
882 (a) Domain structure of AtVAMP714, showing sites of primers used to contruct a negative
883 dominant protein gene.
884 (b) AtVAMP714 Domain DNA sequence and primers used.
885 (c) Domain amino acid sequences.
886 (d) *AtVAMP714* gene expression in dominant negative transgenics.
887 (e) Phenotypes of dominant negative and wildtype plants.
888
889 **Figure S2. VAMP714 expression in Arabidopsis.**
890 (a-e) *proVAMP714::GUS* is expressed in vascular tissues.
891 (a) Whole seedling, 4 dpg, bar = 1 mm.
892 (b) Seedling root, 4 dpg with transverse section in mature region of root, showing GUS
893 activity in the stele (b'), bar = 1 mm.
894 (c) Cotyledon at 4 dpg, bar = 1 mm.

895 (d) root-hypocotyl junction at 4 dpg, bar = 1 mm.
896 (e) primary root tip, 4 dpg, bar = 100 µm.
897 (f) Expression heat map of VAMP714 gene in primary root of Arabidopsis.
898 Visualized using online tool at http://bar.utoronto.ca/eplant/. Red denotes high expression,
899 yellow denotes low expression.
900
901 **Figure S3. Proposed model for the role for VAMP714 in exocytosis and endosomal**
902 **cycling of PIN proteins.**
903 Our data show that VAMP714:mCherry-positive vesicles (purple) move towards the
904 plasma membrane, and co-localize at the plasma membrane (PM) with PIN proteins.
905 VAMP714 also accumulates in BFA bodies and in aggregates following latrunculin B
906 treatment, in the same manner as PIN proteins, both processes being part of endosome
907 recycling (green). VAMP714 is also required for PIN1-positive BFA body formation. It is
908 therefore proposed that VAMP714 is required for both exocytosis of PIN vesicles to the
909 plasma membrane and for PIN cycling between the plasma membrane and endosomes, a
910 process sensitive to BFA and latrunculin B in Arabidopsis.
911
912 **Video S1. VAMP714 localizes to the plasmamembrane via vesicle trafficking.**
913 Video showing time series of VAMP714:mCherry expression (30 images were captured
914 over 10 minutes).
915

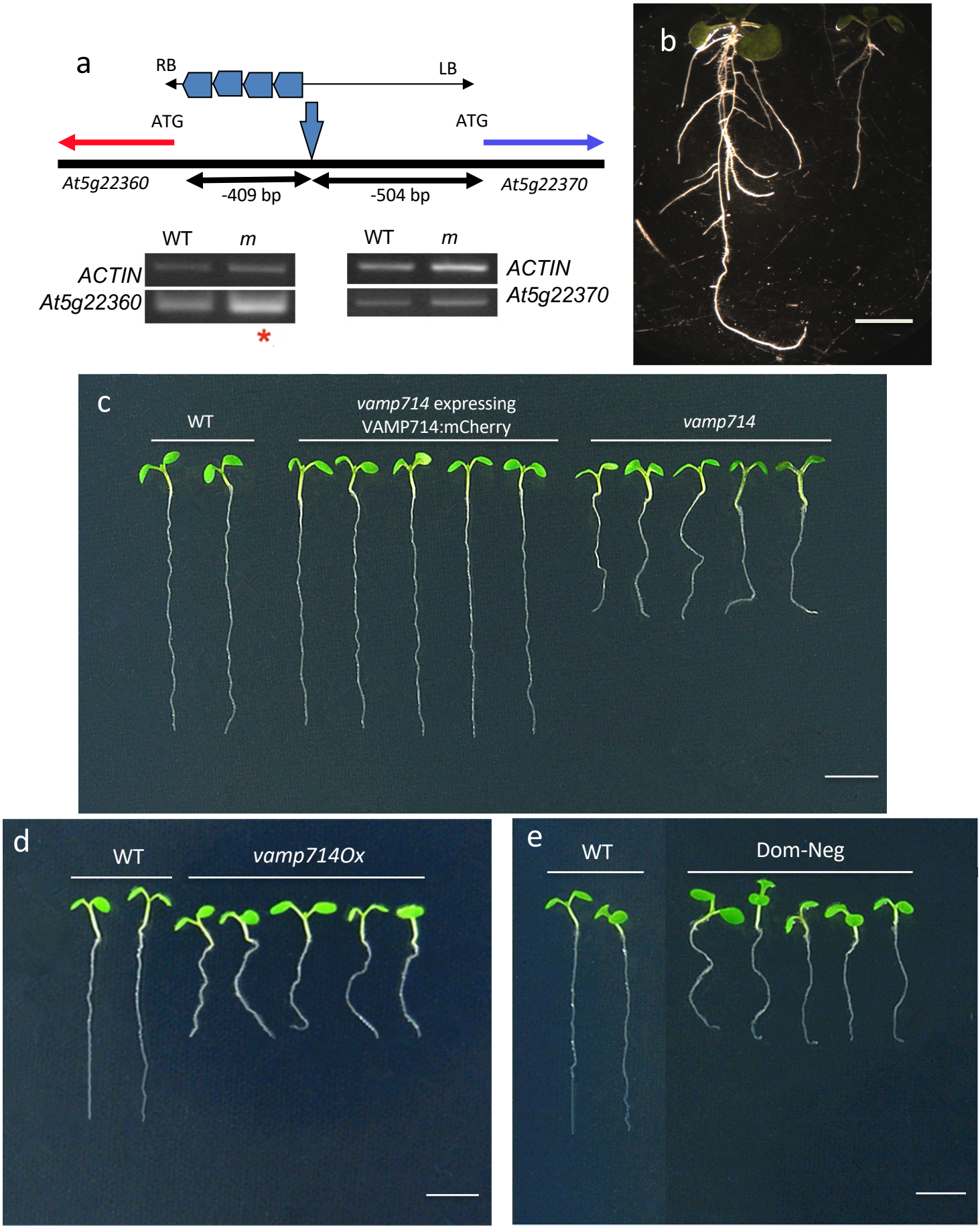
a
RB
LB
ATG
ATG
At5g22360
-409 bp
-504 bp
At5g22370
WT
m
ACTIN
At5g22360
*
WT
m
ACTIN
At5g22370
b
c
WT
vamp714 expressing
VAMP714:mCherry
vamp714
d
WT
vamp714Ox
e
WT
Dom-Neg

Fig. 1

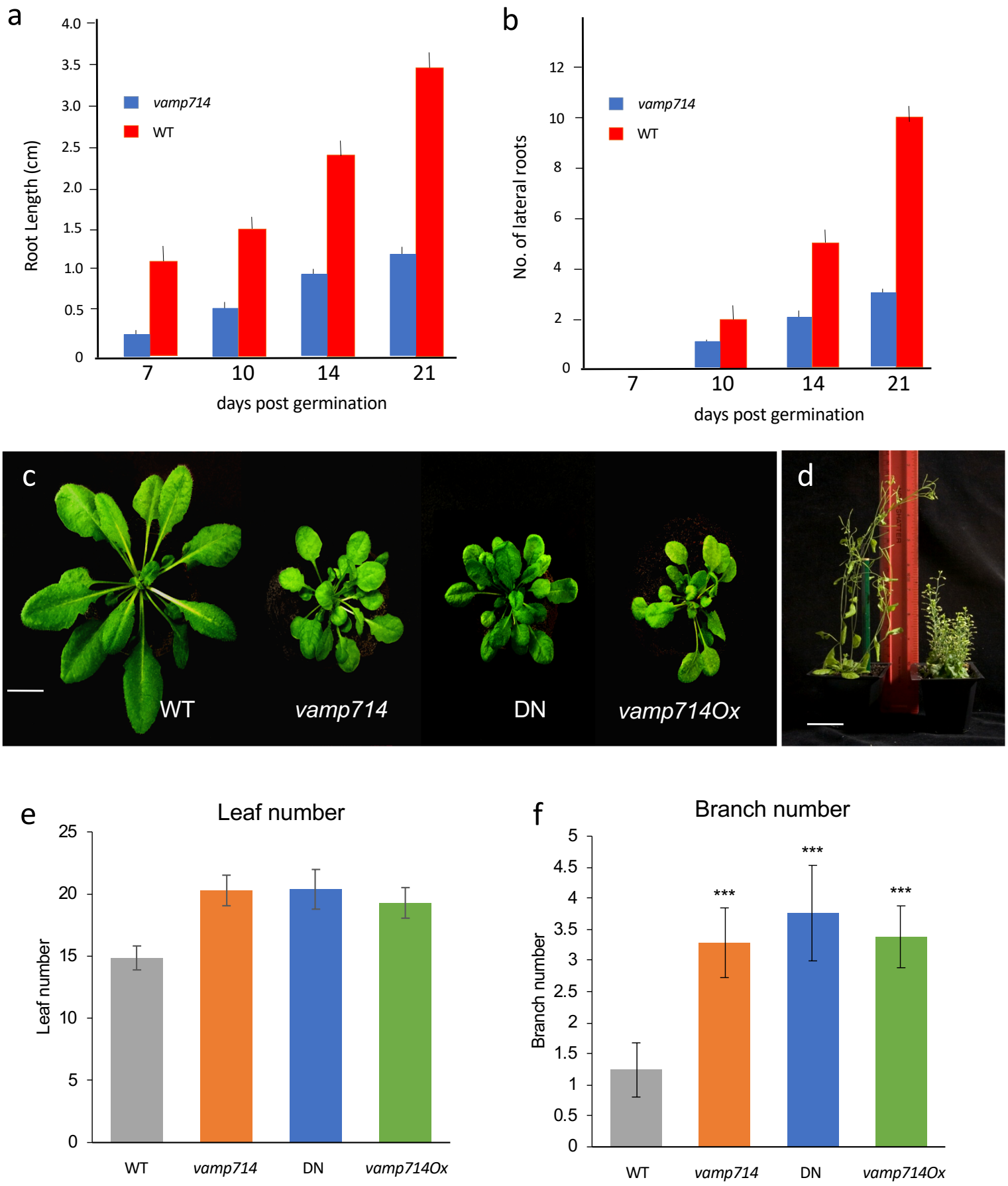
a
Root Length (cm)
4.0
3.5
3.0
2.5
2.0
1.5
1.0
0.5
0
vamp714
WT
7
10
14
21
days post germination
b
No. of lateral roots
12
10
8
6
4
2
0
vamp714
WT
7
10
14
21
days post germination
c
WT
vamp714
DN
vamp714Ox
d
e
Leaf number
Leaf number
25
20
15
10
5
0
WT
vamp714
DN
vamp714Ox
f
Branch number
Branch number
5
4.5
4
3.5
3
2.5
2
1.5
1
0.5
0
***
***
***
WT
vamp714
DN
vamp714Ox

Fig. 2

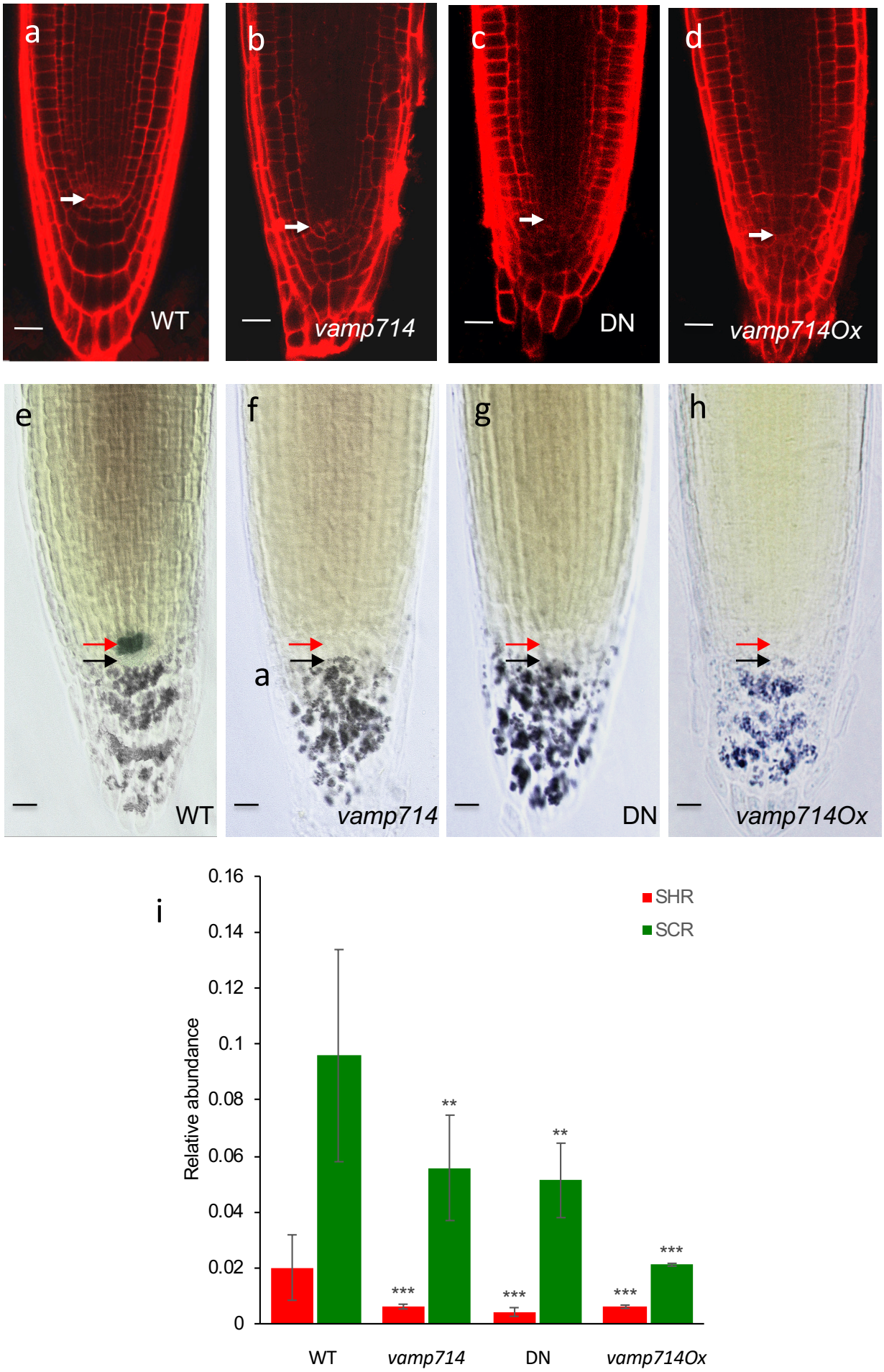
a
WT
b
vamp714
c
DN
d
vamp714Ox
e
WT
f
a
vamp714
g
DN
h
vamp714Ox
i
SHR
SCR
Relative abundance
0.16
0.14
0.12
0.1
0.08
0.06
0.04
0.02
0
**
**
***
***
***
***
WT
vamp714
DN
vamp714Ox

Fig. 3

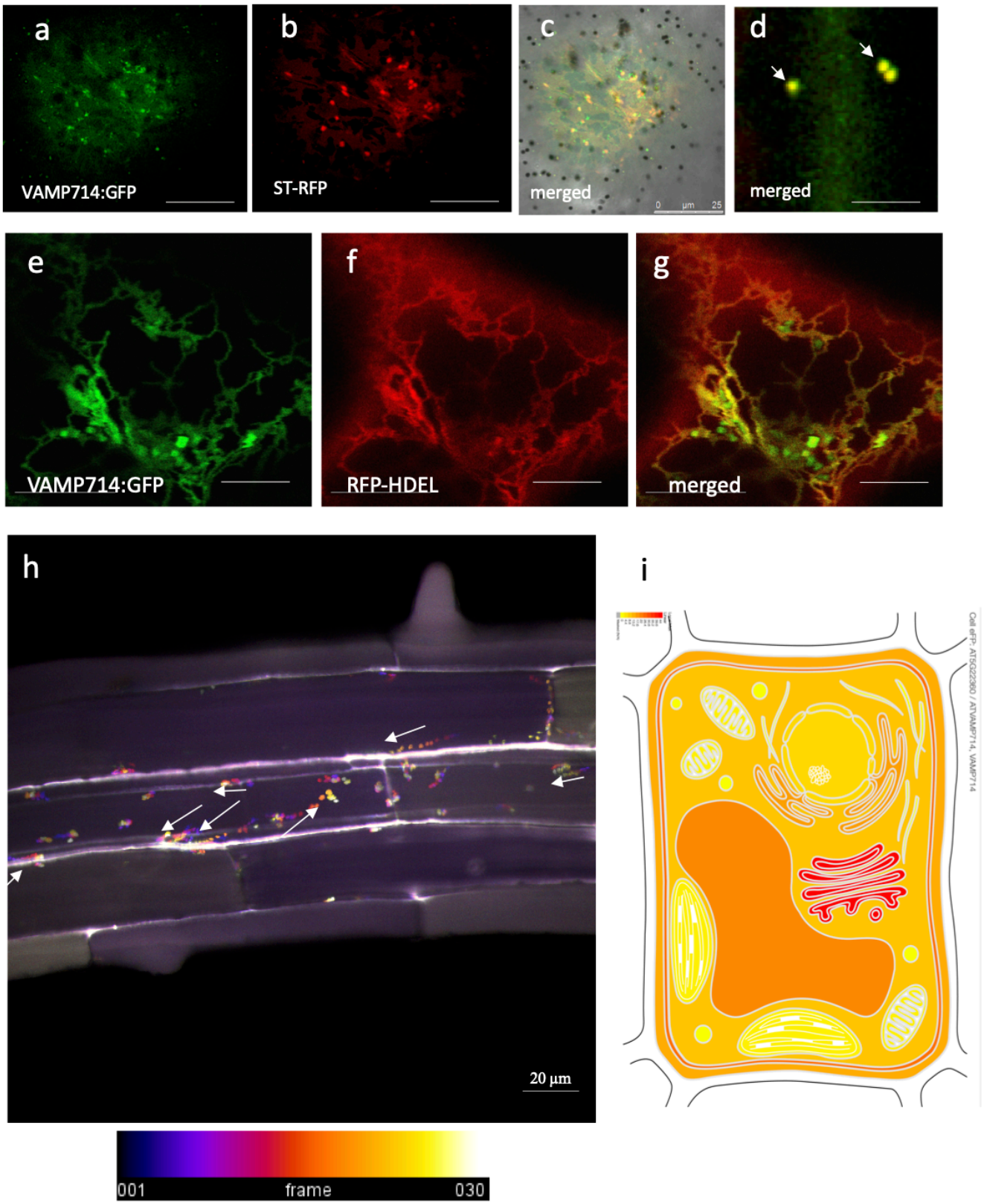
a
VAMP714:GFP
b
ST-RFP
c
merged
d
merged
e
VAMP714:GFP
f
RFP-HDEL
g
merged
h
20 µm
001
frame
030
i

Fig. 4

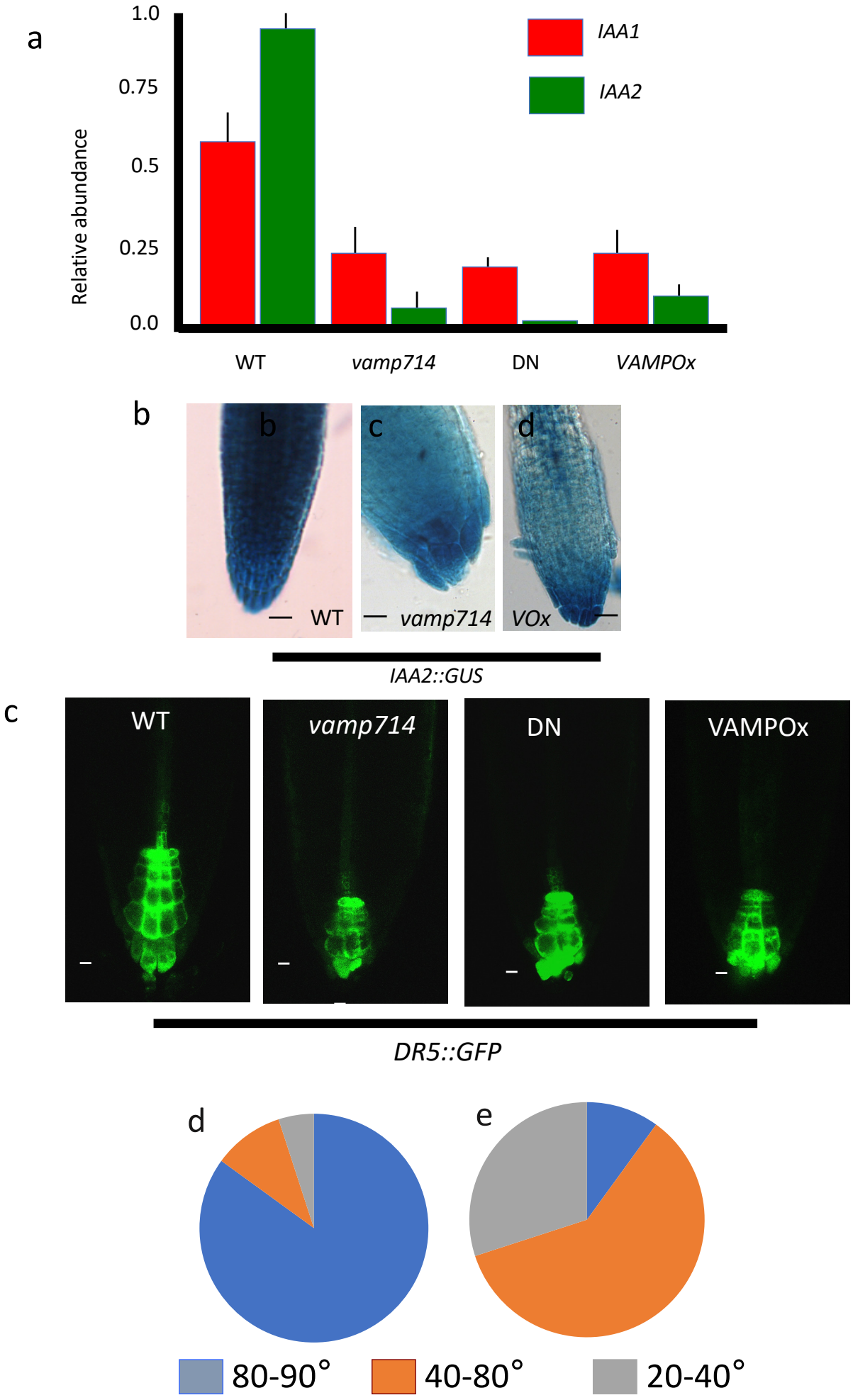
a
1.0
0.75
0.5
0.25
0.0
Relative abundance
IAA1
IAA2
WT
vamp714
DN
VAMPOx
b
b
c
d
WT
vamp714
VOx
IAA2::GUS
c
WT
vamp714
DN
VAMPOx
DR5::GFP
d
e
80-90°
40-80°
20-40°

Fig. 5

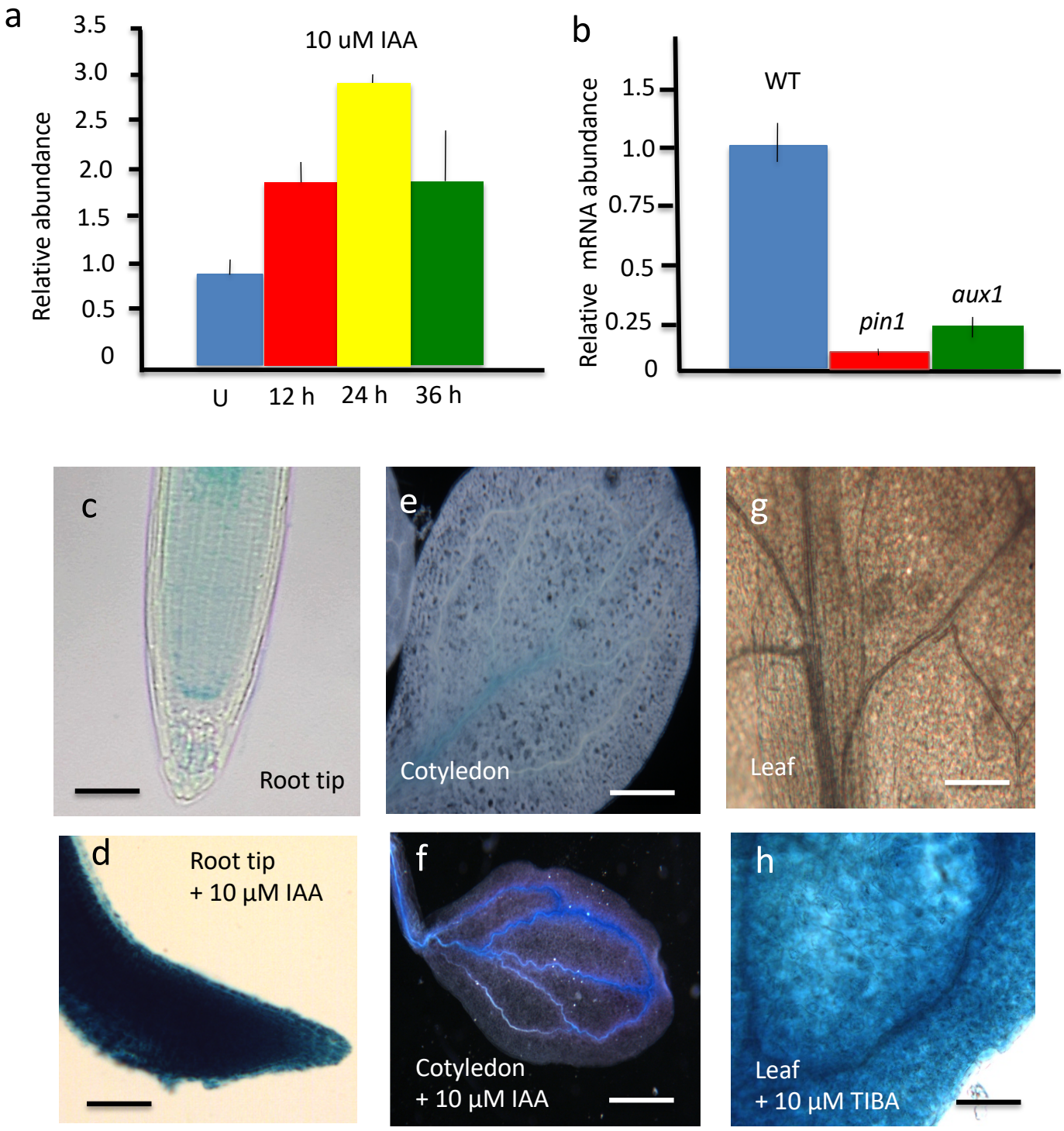
a
10 uM IAA
Relative abundance
3.5
3.0
2.5
2.0
1.5
1.0
0.5
0
U
12 h
24 h
36 h
b
WT
pin1
aux1
Relative mRNA abundance
1.5
1.0
0.75
0.5
0.25
0
c
Root tip
e
Cotyledon
g
Leaf
d
Root tip
+ 10 µM IAA
f
Cotyledon
+ 10 µM IAA
h
Leaf
+ 10 µM TIBA

Fig 6

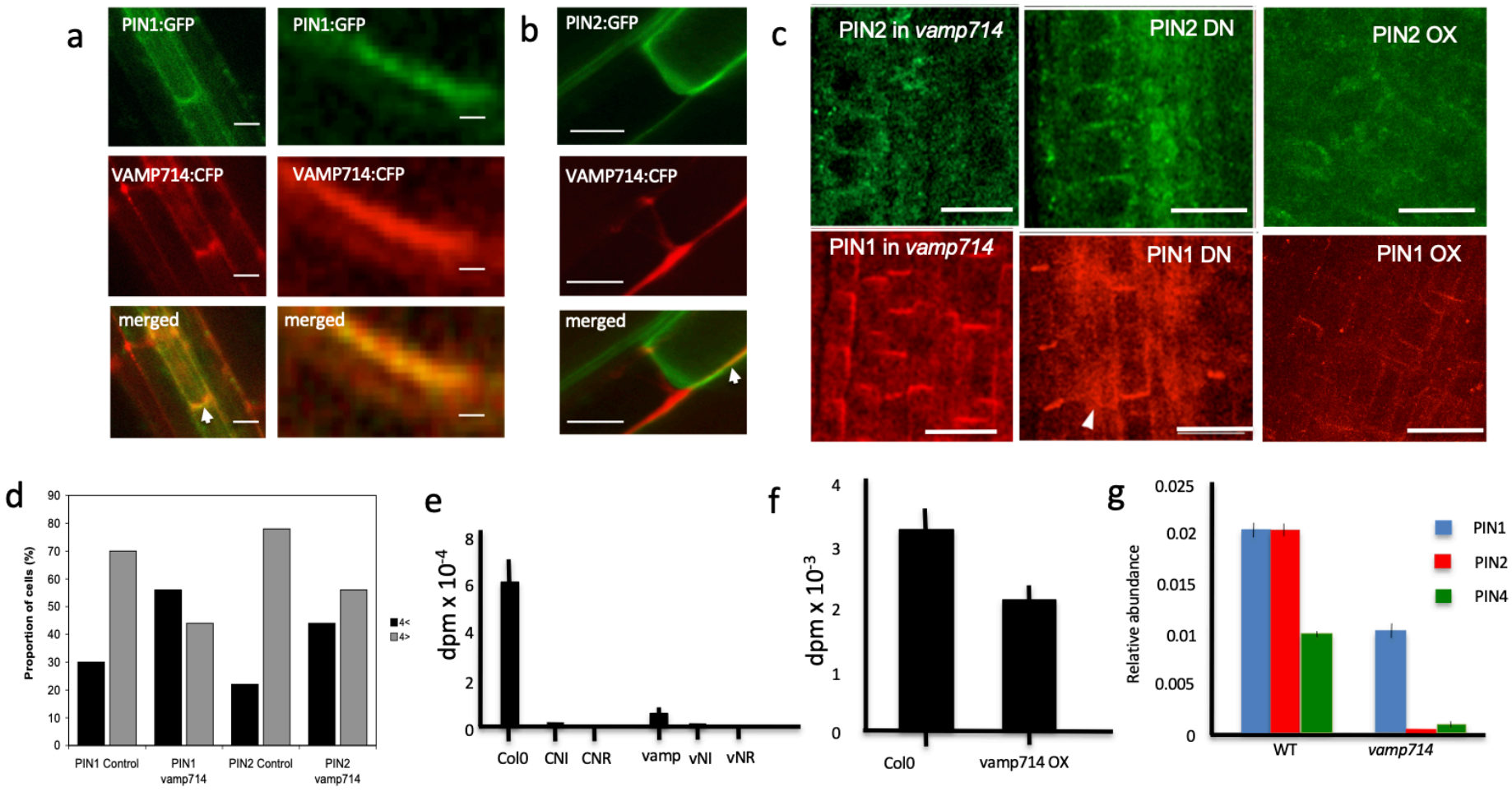
a
PIN1:GFP
PIN1:GFP
VAMP714:CFP
VAMP714:CFP
merged
merged
b
PIN2:GFP
VAMP714:CFP
merged
c
PIN2 in vamp714
PIN2 DN
PIN2 OX
PIN1 in vamp714
PIN1 DN
PIN1 OX
d
Proportion of cells (%)
90
80
70
60
50
40
30
20
10
0
4<
4>
PIN1 Control
PIN1 vamp714
PIN2 Control
PIN2 vamp714
e
dpm x 10-4
8
6
4
2
0
Col0
CNI
CNR
vamp
vNI
vNR
f
dpm x 10-3
4
3
2
1
0
Col0
vamp714 OX
g
Relative abundance
0.025
0.02
0.015
0.01
0.005
0
PIN1
PIN2
PIN4
WT
vamp714

Fig. 7

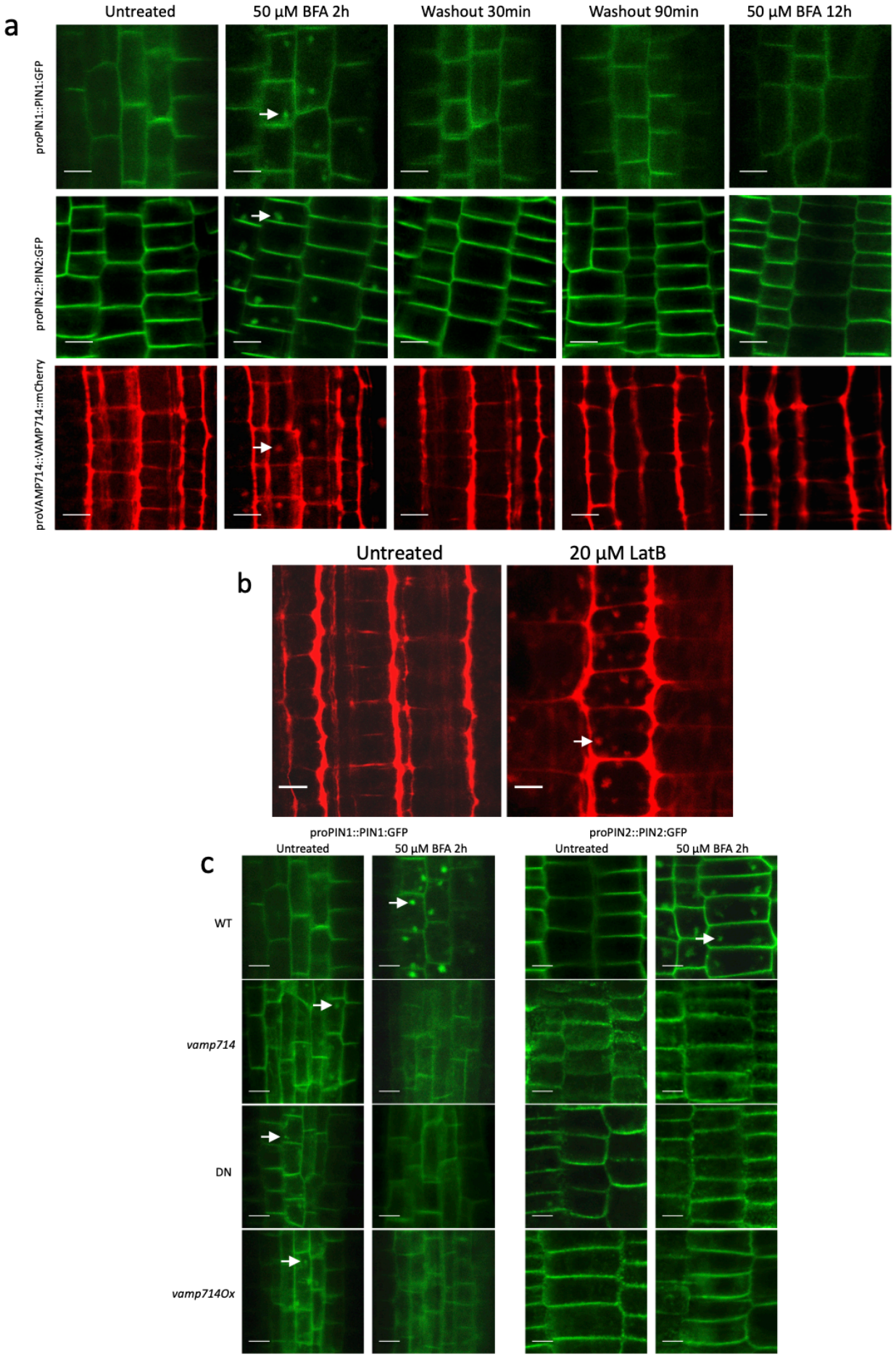
a
Untreated
50 µM BFA 2h
Washout 30min
Washout 90min
50 µM BFA 12h
proPIN1::PIN1:GFP
proPIN2::PIN2:GFP
proVAMP714::VAMP714::mCherry
b
Untreated
20 µM LatB
c
proPIN1::PIN1:GFP
Untreated
50 µM BFA 2h
proPIN2::PIN2:GFP
Untreated
50 µM BFA 2h
WT
vamp714
DN
vamp714Ox

Fig. 8